BARATOVITE–KATAYAMALITE MINERALS FROM THE HODZHA–ACHKAN ALCALINE MASSIF (KIRGIZIA)

Leonid A. Pautov, Vladimir Yu. Karpenko, Atali A. Agakhanov
Fersman Mineralogical Museum, Russian Academy of Sciences, Moscow, Russia, pla58@mail.ru

The baratovite $KLi_3Ca_7Ti_2[Si_6O_{18}]_2F_2$ – katayamalite $KLi_3Ca_7Ti_2[Si_6O_{18}]_2(OH)_2$ mineral series is found in pyroxene-feldspar fenites at the northern contact of the Hodzha-Achkan alkaline massif in Taldy-Bulak valley (a northern slope of the Alaysky ridge, Batkensky Region, Kyrgyzstan). The baratovite-containing rocks have a spotty, striate texture, consertal structure, and a changeable color index that is caused by uneven distribution of the main and minor minerals: hedenbergite – aegirine pyroxenes, microcline, albite, wollastonite, miserite (REE_2O_3 to 5.5 wt.%), calcite (SrO to 1.1 wt.%), quartz. Accessory minerals are: titanite, fluorite, andradite, zircon, turkestanite, ekanite, thorite, tadzhikite-(Ce), britholite group minerals, stillwellite-(Ce), datolite, bazzirite, gittinsite, fluorapatite, barite, galena, molybdenite, pyrite, and pyrrhotite. Baratovite-katayamalite forms lamellar individes to 3 cm with a pinkish color. In short-wave UV-radiation the color is bluish-white. VHN microhardness = 670 (5–6 on the Mohs scale). $D_{meas.}$ = 2.92(2), $D_{calc.}$ = 2.91 g/cm^3. Biaxial, optically positive, 2V from 70° to 90°, dispersion strong, $r > v$; n_g = 1.674(2), n_m = 1.671(3), n_p = 1.666(3). IR spectrum (intensive bands, cm^{-1}): 1082, 972, 695, 598, 570, 541, 521, 478, 448, 412. The X-ray powder data obtained by photomethod (Guinier camera), and diffractometry are given. Parameters of a cell (photomethod): a = 16.93(1), b = 9.742(5), c = 20.92(2)Å, β = 112.51(5)°, V = 3187(5)A^3. Chemical composition of baratovite/katayamalite (wt.%): SiO_2 51.29/51.01; Al_2O_3 0.20/0.06; TiO_2 8.87/7.97; ZrO_2 2.22/3.71; Nb_2O_5 0.00/0.23; SnO_2 1.01/1.87; Fe_2O_3 0.60/0.44; CaO 26.72/26.72; Li_2O^* 3.20/3.17; K_2O 3.17/3.07; Na_2O 0.15/0.23; F 1.75/0.94; H_2O^* 046/0.84; -O=F_2 −0.73/−0.39; total 98.91/98.87 (* – calculated). Most analyses belong to the middle of series between baratovite and katayamalite (F 0.70–1.30 apfu, electron microprobe analysis). The described rocks are close to quartz-albite-aegirine with baratovite-miserite from the Darai-Pioz (Tajikistan), where there is a similar list of accessory minerals (tadzhikite-(Ce), turkestanite, stillwellite-(Ce), bazirite), but there are also some differences: at Hodzha-Achkan, andradite, ekanite, minerals of britholite group are found; pyroxenes are slightly less alkaline, and there are albite pertites in large microcline grains. This occurrence of baratovite is the second in the world and katayamalite the third.
8 tables, 11 figures, 76 references.
Keywords: baratovite, katayamalite, Hodzha-Achkan, Darai-Pioz, Matchaisky intrusive complex.

Introduction

During field work on the Hodzha-Achkan massif (Kyrgyzstan) in 1993, we found samples containing the baratovite-katayamalite mineral series. In 2011, additional material was collected on the same massif, which allowed us to characterize in more detail the minerals of this series, as well as rocks bearing this mineralization.

Baratovite $KLi_3Ca_7Ti_2[Si_6O_{18}]_2F_2$ and its hydroxyl analogue – katayamalite $KLi_3Ca_7Ti_2[Si_6O_{18}]_2(OH)_2$ – are very rare layered titanosilicates with six-membered isolated rings of SiO-tetrahedrons, known earlier only from the type localities. Baratovite was firstly discovered by V.D. Dusmatov and colleagues on the Darai-Pioz (Tajikistan) alkaline massif in the form of nacreous-white lamellar forms to 5×2×0.5 cm in quartz-albite-aegirine pegmatite streaks connected with quartz-containing aegirine syenites, and in albitites of these syenites (Dusmatov *et al.*, 1975). Later the mineral was found in the same massif in other associations: in agrellite-wollastonite-feldspar rocks, in pyroxene-quartz-feldspar rocks with polylithionite (the largest forms of baratovite, up to 7 cm in size, are found there), and in silexytes with leucosphenite, sogdianite, pectolite, polylithionite and reedmergnerite. Katayamalite was described by Nobihude Murakami and coauthors as a new mineral from Ivagi island, Ekhime Pref., in the southwest of Japan, in aegirine syenite, in which it consists of 0.3–0.5 vol.% of the rock. It forms fine tabular grains of white color to 0.5 mm in association with albite, pectolite, wollastonite and sugilite (Murakami *et al.*, 1983). Comparison of associations of the baratovite group minerals from the Darai-Pioz, Ivagi and Hodzha-Achkan are shown in table 1.

Methods of investigation

The mineralogical composition of the baratovite-containing rocks was studied in polished and transparent-polished sections and in crushed samples. Indices of refraction were measured by theodolitic-immersion method with V.G. Feklichev's PPM-1 stage. Both De-

Fig. 1. The geographic location (a) and the geological map (b) of the Turkestano-Alay alkaline massifs (drawn using the Geological map of Tajik SSR and adjacent territories (1984), the Geological map of Kirgiz SSR (1980), and field materials of A.V. Berezansky and V.M. Nenakhov. The rectangle in figure (a) shows the area of the geological map. Digits in circles are the designated massifs, as follows:
1 — Dzhilisu;
2 — Hodzha-Achkan;
3 — Kulpsky;
4 — Utrensky;
5 — Matchinsky;
6 — Upper Darai-Pioz (Darai-Pioz itself);
7 — Middle Dara-Pioz;
8 — Tutek.
The names of intrusive complexes are shown in the map legend according to V.M. Nenakhov et al. (1987).

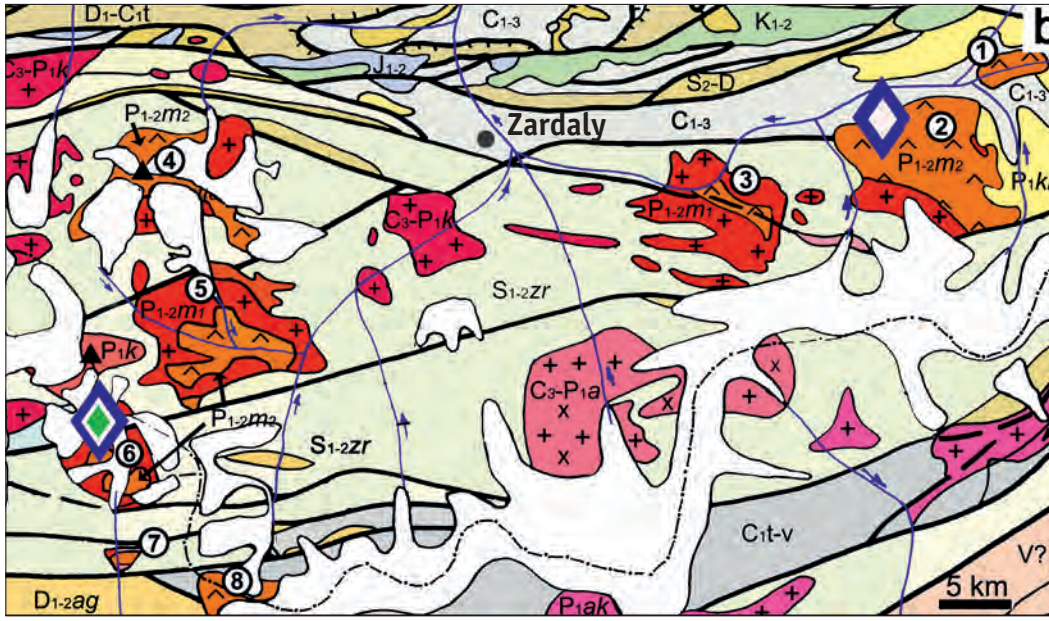

Symbols in the geological map:

Sediment formations:

- K_{1-2} — *Lower — Upper Cretaceous. Speckled sandstones, conglomerates, clays, marls, limestones, gypsums*
- J_{1-2} — *Lower — Middle Jurassic. Speckled sandstones, conglomerates, coals, clays*
- P_1km — *Lower Permian, kumbel series. Red sandstones, conglomerates, rarely — schists*
- C_{1-3} — *Lower — Upper Carbon. conglomerates Sandstones, gravelites, aluerolites, soapstones*
- C_1t-v — *Lower Carbon. Tournai — Vise. Conglomerates, sandstones, limestones, schists*
- D_1-C_1t — *Lower Devonian — Lower Carbon (Tournai). Limestones, dolomites.*
- $D_{1-2}ag$ — *Lower — Middle Devonian, agbalyiskaya series. Tuffs, aluerolites, sandstones, limestones*
- S_2-D — *Upper Silurian — Devonian. Schists, sandstones, limestones, flintstones, porphyrites, tuffs*
- $S_{1-2}zr$ — *Lower—Silurian, zeravshan series. Sandstones, coal-silicious schists, chlorite schists*
- V? — *Vendian(?) Greenschists metamorphites*

Intrusive formations:

- $P_{1-2}m_2$ — *Matchaisky complex. Phase 2. Alkaline and nepheline syenites, syenites, their dikes*
- $P_{1-2}m_1$ — *Matchaisky complex. Phase 2. Alkaline and nepheline syenites, syenites, their dikes*
- P_1k — *Karakyzsky complex. Granodiorites, quartz diorites*
- P_1ak — *Achikalminsky complex. Granites*
- C_3-P_1k — *Karavshinsky complex. Leucogranites , adamellites and their pegmatites*
- C_3-P_1a — *Archabashinsky complex. Granodiorites, quartz monzonites*

Glaciers

Mountains

Baratovite mineral group locations:
1 — Darai-Pioz; 2 — Hodzha-Achkan

bye-Scherrer and Guinier photomethods (with RKD-57.3, DKS-60 and Huber 621 cameras), and diffractometry (DRON-2) were used for X-ray powder data.

The chemical composition of baratovite and of minerals from the baratovite-containing rocks was studied both by electron probe analysis (using wave-dispersive [WDS] and energy-dispersive [EDS] spectrometers) and by wet chemistry. EDS analyses were performed with the CamScan-4D scanning electron microscope, equipped with an EDS (Si-Li) detector (U = 20 kV, I = 4 nA for metallic Co; ISIS Oxford analysis system) and with a JCXA-733 Superprobe JEOL electron microanalyzer, equipped with an EDS (Si-Li) detector with a thin ATW-2 window (U = 20 kV, I = 2 nA; INCA Energy Oxford analysis system). WDS analyses were performed with a JCXA-733 JEOL Superprobe electron microanalyzer with five spectrometers and a Camebax-microbeam with four spectrometers. Measurement conditions on the Camebax-microbeam are as follows: an accelerating voltage of 15 kV; probe current of 20 nA; counting time for main elements is 10 sec at peak, 5 sec at background; counting time for Rb*Lα*, Sr*Lα*, F*Kα* is 40 sec at peak, 20 sec at background. Calculation of concentrations was carried out by means of the of PAP correction program from the device software. The analysis on WDS of JCXA-733 Superprobe JEOL was carried out at an accelerating voltage of 15 kV and 20 kV and probe current of 20 nA. The analysis on fluorine (TAP crystal) and boron (STE crystal) were carried out at an accelerating voltage of 10 kV and probe current of a 30 nA with the beam defocused to 20 microns. The counting time of main elements is 20 sec at the peaks and 10 sec at background; counting time for Rb*Lα*, Sr*Lα*, Sn*Lα*, Hf*Mα* is 50 sec at peak and 20 sec at background; counting time for F*Kα*, B*Kα* is 200 sec at the peaks and 100 sec at background. Standards used are as follows: Si*Kα*, Ca*Kα* — NMNH 164905 Cr-augite; Ti*Kα*, Mn*Kα* — $MnTiO_3$; Zr*Lα* — USNM 117288-3 zircon; Sn*Lα* — SnO_2; Fe*Kα* — Fe_2O_3; Zn*Kα* — ZnO; Mg*Kα* — USNM 143968 pyrope; Sr*Lα* — $SrSO_4$; Cs*Lα* — $Cs_2Nb_4O_{11}$; Rb*Lα* — $Rb_2Nb_4O_{11}$; K*Kα*, Al*Kα* — STD 107 microcline; Na*Kα* — jadeite; F*Kα* — fluor-phlogopite; B*Kα* — danburite and stillwellite-(Ce). Calculation of concentrations was carried out by means of ZAF correction, for F and B — with full PAP correction.

Li and Rb were measured by a flame photometry method (FMD-4 spectrometer of Opton) and optical-emission spectrometry with the inductive coupled plasma method (ICP-OES MPX of Varian). For flame-photometric determination of rare alkalis an acid digestion ($HF + H_2SO_4$) of mineral weights, solubilized at a nitric acid solution has performed. Cs with 1000 ppm of final concentration in solutions was used as the ionization buffer.

F was determined by potentiometer method with an ion-selective electrode. For opening of weights of samples fusion with NaOH in nickel crucibles was used. Water amount was determined from micro-weights by the method of elemental analysis with chromatographic completion (Carlo-Erba 1106 CHN analyzer, carrier gas — helium for chromatography, reactor temperature — 1030°C, a filler of a chromatographic column is Porapak QS). In order to study accessory minerals from crushed samples of rock, the fraction — 100 μm was separated in formyl tribromide (D = 2.89 g/cm^3), and then exposed to magnetic separation. Both EDS qualitative analysis method and powder X-ray methods were used for mineral diagnostics.

Fig. 2. Hodzha-Achkansky massif: a — a general view of the massif from the lower reaches of the Gaumysh river; in the foreground the south-east part of the Dzhilisu massif is visible; b — Taldy-Bulak valley, cutting a contact of syenites with slates in the northern part of the Hodzha-Achkan; the baratovite group minerals are found in its debris cones. Photo: L.A. Pautov.

Mode of occurence

The Hodzha-Achkan massif is at the near-watershed part of the northern slope of the Alaisky ridge at elevations from 2900 to 5100 m (Batken oblast, Kyrgyzstan). The massif is exposed on the left bank of the Hodzha-Achkan River at the headwaters (Fig. 1, 2) between its two left branches (Loisu and Tilbe). It is possible to reach the bottom of the massif by foot from Aidarken (Khaidarkan) settlement through the Gaumysh pass and further down the valley of the Gaumysh river to its confluence with the Hodzha-Achkan river, or from Zardaly (Korgon) kishlak (village), located on confluence of the Ak-Terek and Hodzha-Achkan Rivers. Because of the rugged terrain, the massif is difficult to access (Fig. 2).

The first data on the massif were published by V.N. Weber based on the results of field work in 1910 (Weber, 1934). A detailed description of the Hodzha-Achkan massif was written by A.V. Moskvin and A.A. Saukov based on studies from 1928 as a part of the Pamir expedition of the Academy of Sciences of the USSR (Moskvin, Saukov, 1931; Moskvin, 1932). Subsequently, numerous researchers have been engaged in studying the massif (Dorfman, Timofeev, 1939; Omelyanenko, 1960; Perchuk, Omelyanenko, Shinkarev, 1961; Perchuk, 1964; Shinkarev, 1966; Ilyinsky, 1970; Ifantopulo, 1975; *et al.*), as well as crews from the Southern-Kyrgyz Geological Prospecting Expedition.

The Hodzha-Achkan massif is located in the area of a joining of the Zeravshansky anticlinorium with the Surmetash folded zone which are separated by the Turkestan regional break of deep underlay (Ilyinsky, 1970; Nenakhov *et al.*, 1987). In the plan the massif is close to isomeric, with abruptly falling contacts. In the north the massif breaks through limestone-slate thickness of upper Carbonian, in the east, poorly metamorphized upper Carbonian – lower Permian conglomerates with lenses of sandstones and limestones; in the west, Silurian sand-slate thickness, metamorphized in amphibolite facies; in the south the massif is limited to tectonic contact with Silurian amphibolites (Ilyinsky, 1970).

The Hodzha-Achkan massif is formed by rocks of three phases of implementation. Rocks of the first phase are widespread mainly in the southwest part of the massif. They are composed of leucocratic granites (often tourmalinized) and quartz syenites. Alkaline syenites and nepheline syenites of the second intrusive phase are predominant and distributed throughout the area (up to 75%). Biotite varieties which contact with country rocks are prevalent and pass into aegirine-augite nepheline syenites.

Rocks of the third intrusive phase are composed of leucocratic biotite granites and make up the small dykes in the host rocks and syenites of the central part of the massif (The stratified..., 1982; Nenakhov *et al.*, 1987). According to V.M. Nenakhov and coauthors (1987), the Hodzha-Achkan massif belongs to the matchaisky Permian intrusive complex, which includes also the Darai-Pioz massif,the type location of baratovite (Dusmatov *et al.*, 1975), as well as the Dzhilisuisky, Kulpsky, Matchasuisky, Gerezsuisky, Utrensky, and Tuteksky alkaline massifs (see the map in fig.1). All the massifs mentioned are characterized by a three-phase structure, with the following sequence of rocks: leucocratic granites (frequently tourmalinized), syenites and quartz syenites (nepheline and alkaline syenites), and, last, quartz-bearing syenites and granites. The increased amounts of Li, Ta, Nb, Zr, Be, Sn, Mo, Th and U in comparison with clarks (Dusmatov, 1971; Nenakhov *et al.*, 1987) is a characteristic feature of the matchaisky intrusive complex massifs. The origin of massifs was followed by development of altered rock haloes with infiltration-metasomatic zonality; this was studied at the Hodzha-Achkan and Dzhilisu massifs by L.L. Perchuk, B.I. Omelyanenko and other researchers (Omelyanenko, 1958; 1960; 1961; Perchuk *et al.*, 1961; Perchuk, 1964). Processes of K-Na metasomatism led to the origin of fenitized rocks, with various mineral compositions and textural – structural features (pyroxenes – feldspar, albite – microcline, wollastonite – feldspar).

Description of the baratovite–bearing rocks

Baratovite-bearing rocks were found in the debris cone of the Taldy-Bulak valley, cutting the northern contact of syenites with slates (Fig. 2). The external appearance and mineral composition of these rocks at Hodzha-Achkan is quite close to those baratovite- and miserite-containing quartz-albite-aegirine rocks, most widespread on the Darai-Pioz, in which baratovite was discovered (Fig. 3) and described later in detail (Dusmatov *et al.*, 1975; Reguir *et al.*, 1999), and to baratovite-containing agrellite-wollastonite-pectolite-microcline rocks from the same massif (Semenov, Dusmatov, 1989). As shown below, despite the similarities, there

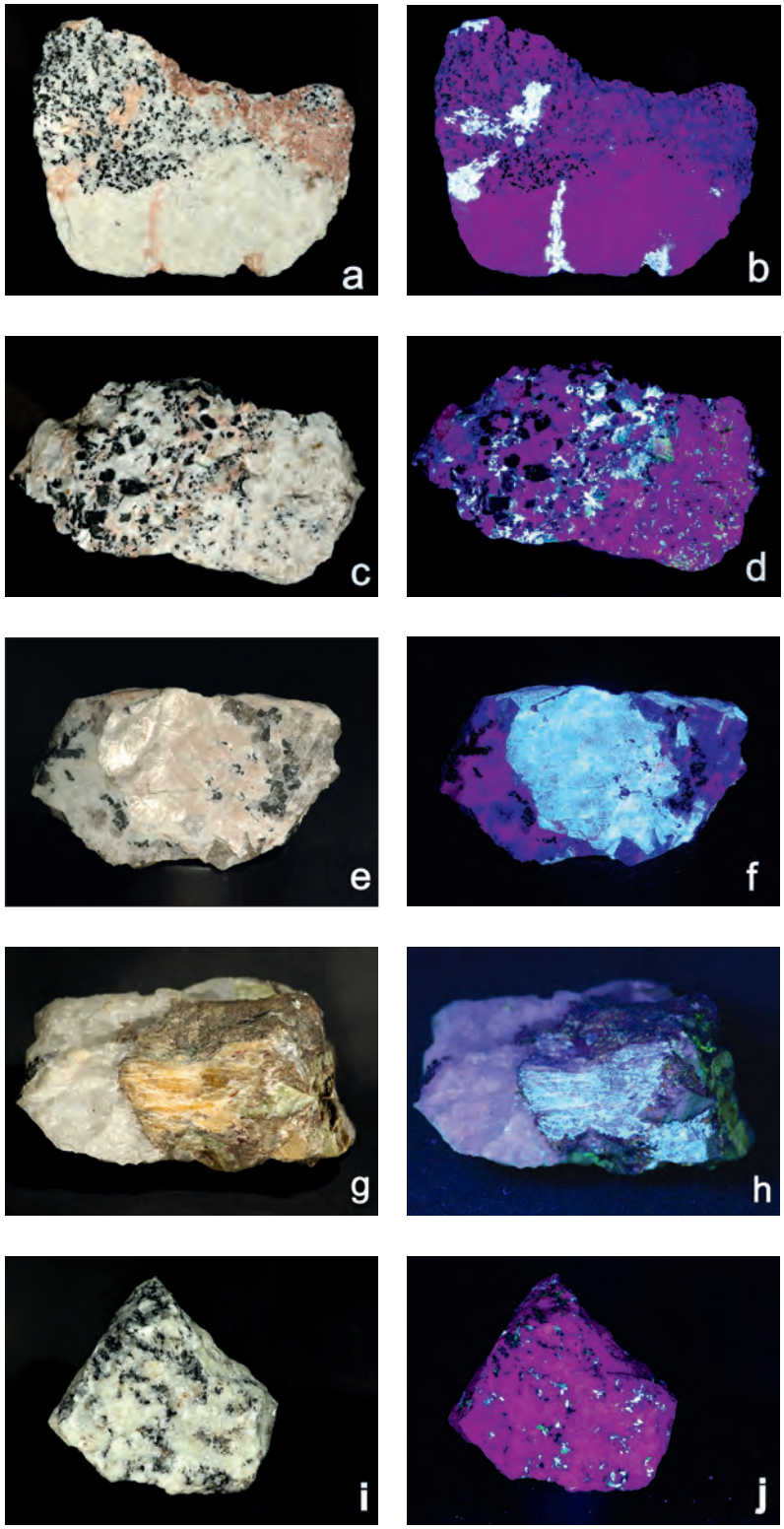

Fig. 3. Baratovite-katayamalite containing rocks: a–d – Hodzha-Achkan (Kyrgyzstan); e–h – Darai-Pioz (Tajikistan) (e, f – baratovite from miserite-pyroxene-feldspar rocks; g, h – baratovite in a silexyte with leucosphenite (green), pectolite agregate (brown). A sample from FMM's funds No. 80873); i – Ivagi (Japan); sample provided by Kotaro Watanabe. On the left – a photo under normal light (pinkish with pearly luster – baratovite, red – miserite); on the right – a photo under short-UV (bluish-white luminescence indicates baratovite group minerals); field of view – 11 cm.

Table 1. **The list of the minerals associated with baratovite and katayamalite**

List of minerals	Formula	Hodzha-Achkan, Kyrgyzstan	Darai-Pioz, Tajikistan Mineral associations					Ivagi, Japan
			Albite - mizerite	Agrellite	Sogdianite - polylithionite	Silexite	Carbonatite	
		1	2	3	4	5	6	7
Zircon	$ZrSiO_4$	+						+
Thorite	$ThSiO_4$	+						
Titanite	$CaTiSiO_5$	+	+	+	+	+	+	+
Andradite	$Ca_3Fe_2(SiO_4)_3$	+						+
Epidote	$Ca_2Al_2Fe^{+3}(SiO_4)_3(OH)$							+
Allanite-(Ce)	$Ce_2Al_3(SiO_4)_3(OH)$							+
Aegirine-hedenbergite	$NaFe^{3+}Si_2O_6$ - $CaFeSi_2O_6$	+ + +	+ + +	+ +	+ + +	+ +	+ +	+ +
Agrellite	$NaCa_2Si_4O_{10}F$			+ + +				
Wollastonite	$CaSiO_3$	+ + +*	+	+ + +				
Miserite	$(K,□)_{1.5}(Ca, REE)_6[Si_8O_{22}](F,OH)_2 \cdot nH_2O$	+ +*	+ +	+ +			+ +	
Pectolite	$NaCa_2Si_3O_8(OH)$	+ ?		+ +	+ +	+ +		+ +
Turkestanite	$Th(Ca,Na)_2(K_{1-},□_X)\ Si_8O_{20} \cdot nH_2O$	+	+	+	+	+		
Ekanite	$ThCa_2Si_8O_{20}$	+						
Datolite	$CaBSiO_4(OH)$	+	+		+			
Fluorcalciobritholite	$(Ca, REE)_5(SiO_4,PO_4)_3F$	+						
Fluorbritholite-(Ce)	$(Ce,Ca)_5(SiO_4,PO_4)_3F$	+						
Tadzhikite	$Ca_3(REE,Y)_2TiB_4Si_4O_{16}O_{22}(OH)_2$	+	+		+	+		
Eudialyte (group)					+	+ +		
Stillwellite-(Ce)	$CeBSiO_5$	+	+		+	+ +	+	
Baratovite	$KCa_7Ti_2Li_3Si_{12}O_{36}(F,OH)_2$	+	+	+	+	+	+	
Katayamalite	$KCa_7LiTi_2(Si_6O_{18})_2(OH,F)_2$	+	+ ?	+ ?	+ ?		+	+
Aleksandrovite	$KCa_7Sn_2Li_3Si_{12}O_{36}F_2$						+	
Faizievite	$K_2Na(Ca_6Na)Ti_4Li_6Si_{24}O_{66}F_2$					+		
Bazirite	$BaZrSi_3O_9$	+	+				+	
Gittinsite	$CaZrSi_2O_7$	+						
Zektzerite	$NaLiZrSi_6O_{15}$				+	+		
Sugilite	$K\ Li_3Na_2Fe^{3+}{}_2Si_{12}O_{30}$				+	+		+ +
Sogdianite	$KLi_3Zr_2Si_{12}O_{30}$				+ +	+ +	+	
Zeravshanite	$Cs_4Na_2Zr_3(Si_{18}O_{45}) \cdot (H_2O)_2$					+		
Leucosphenite	$BaNa_4Ti_2B_2Si_{30}$				+ +	+ +		
Annite	$KFe_3AlSi_3O_{10}(OH)_2$	+						
Polylithionite	$KLi_2AlSi_4O_{10}F_2$				+ +	+ +		
Sokolovaite	$CsLi_2AlSi_4O_{10}F_2$					+		
Orlovite	$KLi_2TiSi_4O_{10}(OF)$					+		
Neptunite	$KNa_2Li(Fe,Mn)_2Ti_2Si_8O_{24}$					+		
Pekovite	$SrB_2Si_2O_8$					+		
Fluorapophyllite	$KCa_4Si_8O_{20}(F,OH) \cdot 8H_2O$					+		
Kapitsaite-(Y)	$(Ba,K)_4(Y,Ca)_2[Si_8(B,Si)_4O_{28}]F$					+		
Microcline	$KAlSi_3O_8$	+ + +	+ + +	+ + +	+ + +	+ +	+ +	+ +
Albite	$NaAlSi_3O_8$	+ + +	+ +	+ +	+ +	+	+	+ + +
Reedmergnerite	$NaBSi_3O_8$				+ +	+ +		
Quartz	SiO_2	+ +	+	+	+ + +	+ + +	+	+ +
Pyrochlore	$(Ca,Na)_2Nb_2O_6(OH)$		+		+	+	+	
Calcite	$CaCO_3$	+ +*	+	+	+ +	+	+ + +	
Fluorapatite	$Ca_5(PO_4)_3F$	+	+		+	+	+	+
Barite	$BaSO_4$	+						
Fluorite	CaF_2	+	+	+	+ +	+	+	
Galenite	PbS	+				+		
Molybdenite	MoS_2	+						
Pyrite	FeS_2	+						
Pyrrhotite	$Fe_{1-x}S$	+						
Bismuth	Bi					+		
Sphalerite	ZnS					+		
Löllingite	$FeAs_2$					+		

Note: +++ − rock forming minerals, ++ − minor, + − accessory; +++ − in different rock types the rock forming mineral can be the main species, or a minor component; ++* − in different rock types the mineral can be either minor or accessory; ? − additional diagnostics of the mineral are required.*
The chart is based on our data as well as additional references (Ryzhev, Moleva, 1960; Ulyanov, Ilyinsky, 1964; Dusmatov et al., 1975; Semenov, Dusmatov, 1989; Murakami, 1976; Murakami et al., 1983; Belakowski, 1991; Reguir et al., 1999; Agakhanov et al., 2011).

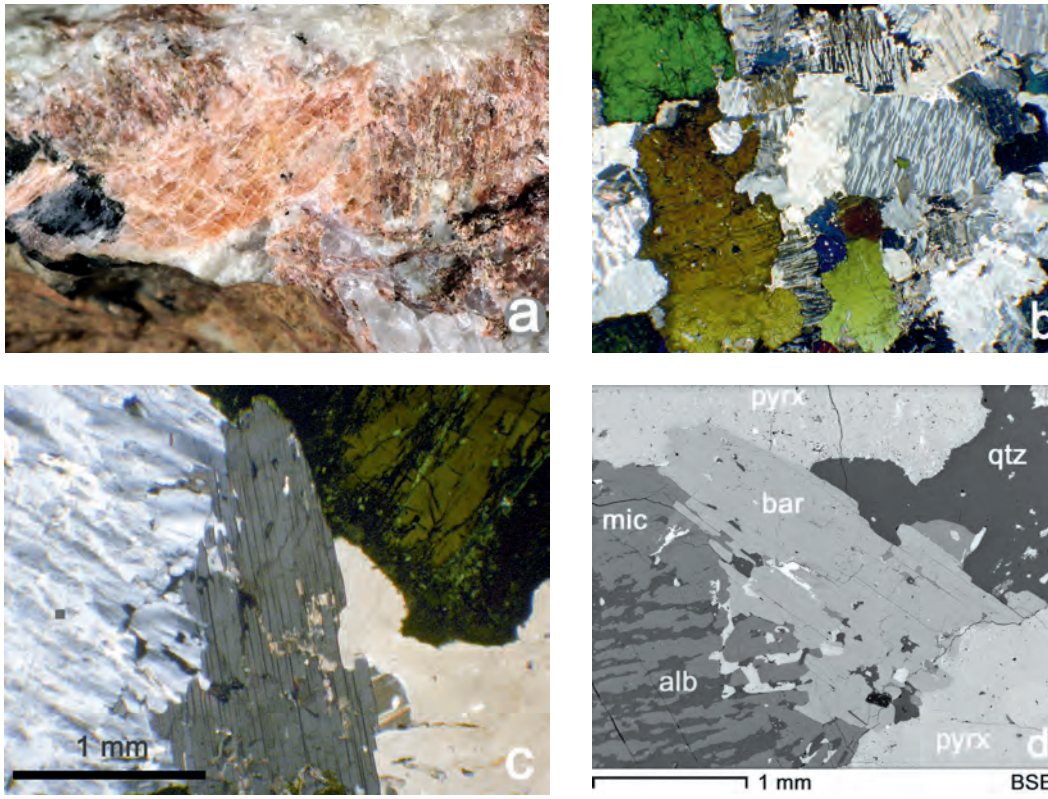

Fig. 4. Baratovite from the Hodzha-Achkan massif:
a — large lamellar form of baratovite (orange-pink) with miserite (darker, brownish-red) in microcline (light gray) with clinopyroxene (black), Taldy-Bulak valley, Hodzha-Achkan; field of view — 2.5 cm;
b — feldspar-pyroxene rock (thin section, crossed nicols). Serpiginous borders of clinopyroxene (green) and microcline-perthite accretion are visible. Grains with indigo-blue interference color are baratovite; field of view — 11 cm.
c — baratovite in feldspar-pyroxene rock (transmitted light, crossed nicols); baratovite is the bluish-grey grain in the center; on the right — microcline-perthite, dark green — clinopyroxene, with the external rim (the dark zone on the periphery of the grain) saturated with small isolated areas of garnet and more alkaline (in contrast to the host grain) pyroxene (aegirine); yellowish on the right — quartz; field of view — 2 mm;
d — the same fragment of a section, turned slightly counterclockwise, BSE mode image; bar — baratovite, pyrx — clinopyroxene; mic — microcline; alb — albite; qtz — quartz; the white extended form in baratovite — fluorcalciobritholite; light-grey grains on the left of the baratovite and microcline-perthite boundary — fluorite; light scattering in the rim zones of clinopyroxene grains — andradite, more dark scattering — aegirine.

are also differences between Hodzha-Achkan and Darai-Pioz baratovite-bearing rocks. Comparison of the mineralogical composition of baratovite- and katayamalite-containing rocks of the Hodzha-Achkan, Darai-Pioz and Ivagi are shown in table 1.

The largest and most abundant baratovite aggregates on the Hodzha-Achkan massif are found in quartz-aegirine-albite-microcline rocks, often with miserite and variable amounts of calcite, wollastonite, titanite, datolite. The color index, texture and structure of such rocks is extremely changeable even within one mass (sample). Spotty texture and, rarely, striate texture are most typical of these rocks. The textures are caused by the presence in leucocratic fine-grained quartz-albite-microcline rock (sometimes with miserite and aegirine), of segregations, consisting of more coarse-grained aggregates of the same minerals, but often in other ratios (Fig. 3). In some varieties of such rocks, miserite is not an accessory or minor mineral, but the main constituent of the rock, giving it a saturated pink color. The leucocratic fine-grained main skeleton of the rock is composed generally of *albite* and nonperthitic *microcline*, approximately in equal proportions; minor minerals include quartz and calcite. The total amount of clinopyroxene and miserite is quite variable samples both enriched and totally deprived colored minerals may be

seen. The coarse-grained aggregates form isomeric, elongated or irregular clusters, which are composed of light-gray microcline-perthite tabular grains (albite perthites occupy 40–50 vol.% of individual K-feldspar grains) (Fig. 4, 5), dark green grains of clinopyroxene (Fig. 4); and variable quantities of calcite, quartz, wollastonite, and miserite. *Clinopyroxene* forms, as a rule, grains with wavy, rough borders and no evidence of crystallographic shape (Fig. 4). Pyroxene compositions (Table 2) are quite close to those from the Darai-Pioz baratovite-containing fenites and have less aegirine than Ivagi pyroxene, also considerably differing from the clinopyroxene composition of the Hodzha-Achkan syenites (Fig. 6). A characteristic feature of clinopyroxene (average composition is $Hd_{64}Aeg_{21}Di_{14}$) from coarse-grained aggregations on the contact with perthitic potassium feldspar is a zone, almost non-transparent in normal thick sections, containing numerous small pores, irregular *garnet* aggregates of andradite composition ($And_{94}Sch_3Gros_2Spes_1$) with smooth outlines and sizes to 15–20 μm (Table 2, analysis 7, 8), and segregations of pyroxene enriched with aegirine (Fig. 4, 7) which do not have crystallographic restrictions. Similar zones in the external rims of pyroxene crystals in alkaline rocks from other regions have been interpreted in the literature as a product of reactionary substitution of earlier high-calcic pyroxene against increased activity of alkalis and fugacity of oxygen (Dawson, Hill, 1988; Marks *et al.*, 2003). However, this has never been noted in baratovite-katayamalite bearing rocks of the Darai-Pioz and Ivagi. Clinopyroxenes without such rims from fine-grained quartz-albite-microcline rock from the Hodzha-Achkan are more alkaline (average composition $Aeg_{44}Hd_{36}Di_{20}$, fig. 6; table 2, analysis 5). A characteristic mineral of the baratovite-containing rocks both of Hodzha-Achkan and Darai-Pioz is miserite (Semenov *et al.*, 1973; Dusmatov *et al.*, 1975; Reguir *et al.*, 1999); as noted above, its presence is subject to considerable variation. *Miserite* at Hodzha-Achkan has been described on multiple occasions: in wollastonite-pyroxene-feldspar

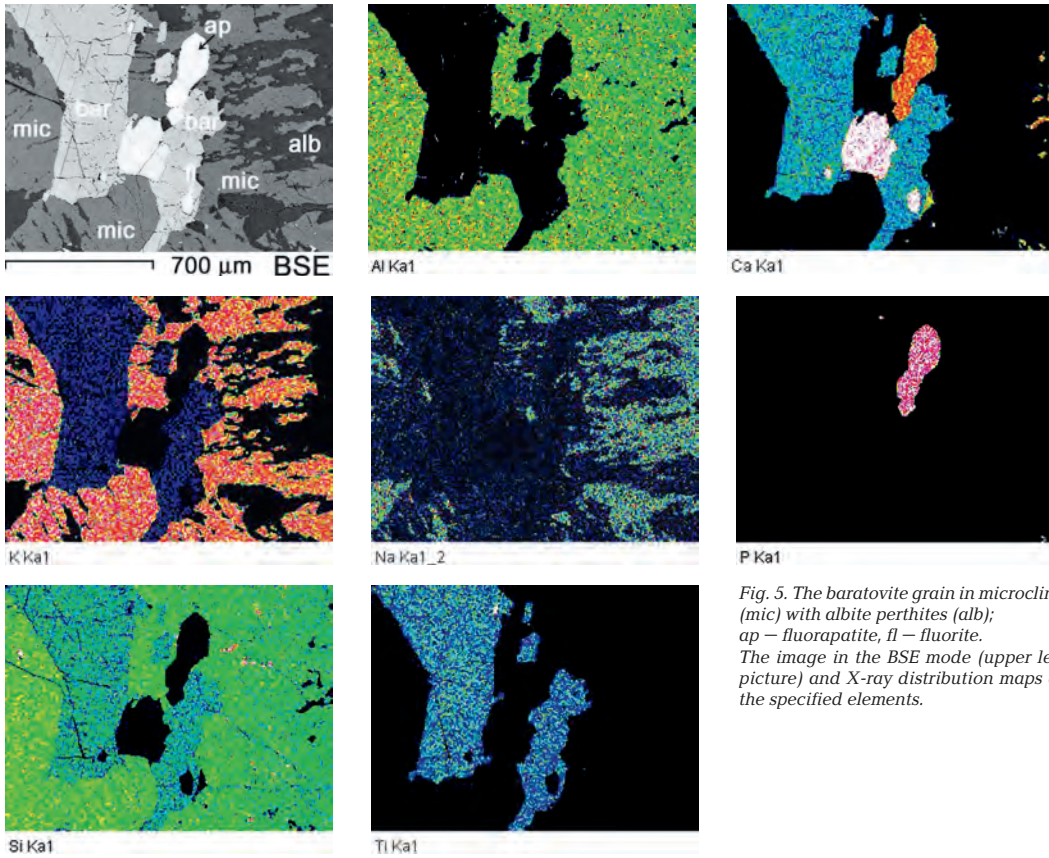

Fig. 5. The baratovite grain in microcline (mic) with albite perthites (alb); ap – fluorapatite, fl – fluorite. The image in the BSE mode (upper left picture) and X-ray distribution maps of the specified elements.

Table 2. **Chemical composition of clinopyroxenes (1–5), wollastonite (6), andradite (7, 8), datolite (9) from the baratovite – containing rocks, Hodzha-Achkan**

Component	1	2	3	4	5	6	7	8	9
SiO_2	50.32	50.93	52.51	53.14	51.75	51.52	35.76	34.62	36.79
TiO_2	0.00	0.15	0.00	0.00	0.11	0.00	0.18	0.00	0.00
Al_2O_3	0.37	0.26	0.27	0.54	0.35	0.00	2.47	0.95	0.00
Fe_2O_3	7.85	7.21	18.55	31.81	14.65	0.00	27.53	31.24	0.00
FeO	18.29	18.84	4.03	1.08	9.94	0.74	0.00	0.00	0.36
MnO	0.60	0.60	1.24	0.17	1.38	0.31	0.38	0.11	0.00
MgO	2.45	2.30	4.47	0.00	3.36	0.00	0.00	0.00	0.00
CaO	18.82	17.64	12.75	0.34	13.25	47.47	33.01	33.38	34.07
Na_2O	2.76	3.21	7.16	13.34	5.97	0.00	0.00	0.00	0.00
Total	100.67	100.41	99.12	97.23	99.29	100.04	99.57	99.93	98.06
				Calculated on the basis of:					
				O = 6 apfu			O = 3 apfu	O = 12 apfu	
Si^{+4}	1.98	2.01	1.99	2.02	2.00	1.00	3.00	2.93	
Al^{+3}	0.02	0.01	0.01	0.02	0.02	0.00	0.24	0.10	
Ti^{+4}	0.00	0.00	0.00	0.00	0.00	0.00	0.01	0.00	
Fe^{+3}*	0.23	0.21	0.53	0.91	0.43	0.00	1.74	1.99	
Fe^{+2}*	0.60	0.62	0.13	0.03	0.32	0.01	0.00	0.00	
Mn^{+2}	0.02	0.02	0.04	0.01	0.05	0.01	0.03	0.01	
Mg^{+2}	0.14	0.13	0.25	0.00	0.19	0.00	0.00	0.00	
Ca^{+2}	0.79	0.74	0.52	0.01	0.55	0.99	2.96	3.02	
Na^{+}	0.21	0.25	0.53	0.99	0.45	0.00	0.00	0.00	
O^{-2}	6.00	6.00	6.00	6.00	6.00	3.00	12.00	12.00	

*Note: * – Fe^{+2}/Fe^{+3} calculated.*
In the following, if there are no special comments analysis was performed by EPMA EDS.
1 – 4 – clinopyroxene from coarse-grained areas of the rock:
1, 2 – the central part of grains; 3 – aegirine isolates from the external rims; 5 – clinopyroxene from fine-grained sites; 6 – wollastonite from coarse-grained wollastonite-pyroxene-feldspar rock; 7, 8 – andradite (calculated on O = 12 apfu): 7 – apple-green grains in the matrix of a rock; analysis sum includes Nb_2O_5 = 0.24 wt. % (corresponds to Nb = 0.01 apfu); 8 – andradite from garne-aegirine rims of a coarse-grained clinopyroxene; 9 – datolite (calculated on the basis of total cations = 2 apfu): $(Ca_{0.99}Fe_{0.01})BSiO_4(OH)$, calculated amounts (wt. %): B_2O_3 = 21.31, H_2O = 5.53.
In the following tables, 0.00 means that the component amount is lower than the limit of detection.

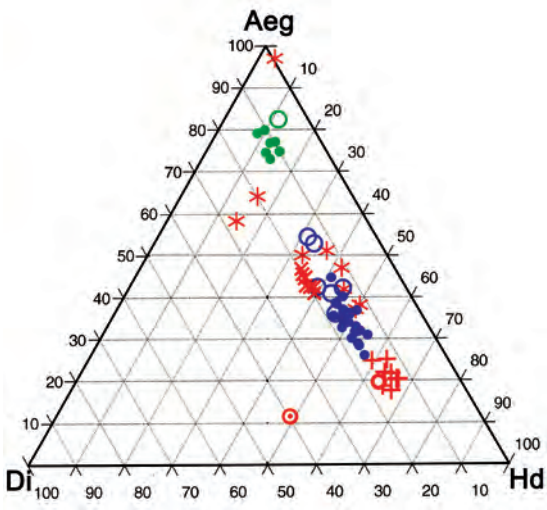

Fig. 6. Chart of clinopyroxene compositions (mol. %) from the baratovite – containing rocks from Hodzha-Achkan:
+ – coarse grains,
∗ – alkaline pyroxene segregations from the external rim of those grains,
× – small grains from fine-grained areas of the feldspar rock (our data);
○ – from quartzless syenites (Perchuk, 1964),
⊙ – from quartz syenites (Perchuk, 1964);

Darai-Pioz (miserite – bearing quartz-albite-microcline rocks):
● – our data,
○ – (Reguir et al., 1999);

Ivagi (aegirine syenite):
● – our data;
○ – Murakami et al., 1983.

Ternary tops correspond to:
Di – diopside, Hd – hedenbergite, Aeg – aegirine.

rocks in the east area (the left bank of the Loisu river) (Ryzhev, Moleva, 1960); in the northwest part of the massif (the valley of Karagach-Dzhilga) at the contact of nepheline syenites with native slates (Ul'yanov, Ilyinsky, 1964); and in albite-pyroxene metasomatites from a talus at the northern contact of the massif (Enikeeva *et al.*, 1987). Aside from Hodzha-Achkan and Darai-Pioz, miserite is known from other massifs of the matchaisky complex: Matchinsky, Kulpsky, Dzhilisuisky (Ilyinsky, 1970; Ifantopulo, 1975). Miserite in other regions of the world is also found in alkaline metasomatites (fenites) with potassium specialization, in alkaline intrusions, or in carbonatites. Other occurrences of miserite include: the contact of metamorphized slates and nepheline syenites in Wilson Springs, Arkansas, USA (Shaller, 1950); aegirine-albite-microcline metasomatites at Chergilen, Khabarovsky krai, E. Siberia (Kupriyanova, Vasilyev, 1961); the contact of dykes of alkaline rocks with limestones at Talassky ridge, Kyrgyzstan (Kozlova, 1962); aegirine − microcline metasomatites in the Yakokutsky massif, Yakutia (Kravchenko, Bykova, 1967); Kipawa carbonatites with wollastonite, orthoclase, aegirine, agrellite, Canada (Berry *et al.*, 1971; Scott, 1976); and fenites of the Murunsky complex, Yakutia (Lazebnik, Lazebnik, 1981; Konev *et al.*, 1996). Miserite at Hodzha-Achkan forms both separate acicular crystals and radial or fanlike aggregates up to 3 cm in size in rock. The color of miserite ranges from pink to saturated henna-red, and is related to the degree of manganese enrichment (MnO to 1.3 wt.%) (Fig. 3a, c). Miserite is the most important concentrator of *REE* in baratovite − bearing rocks at Hodzha-Achkan. Unlike miserite at Darai-Pioz, which is characterized by an increased dominance of yttrium *REE*, Hodzha-Achkan miserite is poor in yttrium and highly enriched in light lanthanides (Table 3). All microprobe analyses of miserite, as a rule, has a low totals, connected with the presence in the mineral of variable amounts of molecular water (Scott, 1976; Rozhdestvenskaya, Evdokimov, 2006). Very difficult mechanisms of isomorphous substitutions occur in miserite, and the idealized formula $KCa_5\square(Si_2O_7)(Si_6O_{15})(OH)F$, proposed by J. Scott (Scott, 1976), and sometimes seen elsewhere in the mineralogical literature, is not electroneutral, and carries a (-3) charge.

Other minerals which in some rock varieties become rock-forming are wollastonite, calcite, and quartz. *Wollastonite* consists of less than 1 vol.% in one type of rock, while in the others

Table 3. **Chemical composition of miserite from Hodzha-Achkan (1−3) and Darai-Pioz (4, 5) massifs (wt.%)**

Component	Hodzha-Achkan			Darai-Pioz	
	1	2	3	4	5
SiO_2	50.30	50.26	49.80	49.16	49.93
TiO_2	0.00	0.22	0.12	0.22	0.30
ZrO_2	0.00	0.00	0.63	0.38	0.31
Nb_2O_5	0.00	0.00	0.31	0.77	0.54
Al_2O_3	0.00	0.00	0.06	0.00	0.00
Y_2O_3	0.00	0.00	0.44	0.59	0.93
La_2O_3	1.29	0.33	0.26	1.16	0.32
Ce_2O_3	3.06	0.90	0.68	2.25	1.20
Pr_2O_3	0.55	0.23	0.00	0.00	0.00
Nd_2O_3	0.59	0.51	0.32	0.45	0.31
MnO	0.00	0.42	0.48	0.15	0.14
FeO	0.25	0.30	0.35	0.20	0.28
CaO	32.88	35.08	34.13	32.18	33.46
Na_2O	0.00	0.16	0.00	0.00	0.00
K_2O	5.99	6.43	6.34	5.94	6.19
F	2.68	2.48	2.79	2.93	3.15
$-O=F_2$	–1.12	–1.04	–1.17	–1.23	–1.32
Total	97.59	97.32	96.71	96.38	97.06
Calculated on the basis of Si + Al = 8 apfu					
K^+	1.22	1.31	1.30	1.23	1.27
Na^+	0.00	0.05	0.00	0.00	0.00
Σ	1.22	1.36	1.30	1.23	1.27
Ca^{+2}	5.60	5.98	5.87	5.61	5.74
Mn^{+2}	0.00	0.06	0.07	0.02	0.02
Fe^{+2}	0.03	0.04	0.05	0.03	0.04
Y^{+3}	0.00	0.00	0.04	0.05	0.08
La^{+3}	0.08	0.02	0.02	0.07	0.02
Ce^{+3}	0.18	0.05	0.04	0.13	0.07
Pr^{+3}	0.03	0.01	0.00	0.00	0.00
Nd^{+3}	0.03	0.03	0.02	0.03	0.02
Nb^{+5}	0.00	0.00	0.02	0.06	0.04
Ti^{+4}	0.00	0.03	0.01	0.03	0.04
Zr^{+4}	0.00	0.00	0.00	0.03	0.02
Σ	5.95	6.22	6.14	6.06	6.09
Si^{+4}	8.00	8.00	7.99	8.00	8.00
Al^{+3}	0.00	0.00	0.01	0.00	0.00
ΣT	8.00	8.00	8.00	8.00	8.00
F^-	1.35	1.25	1.42	1.51	1.60
O^{-2}	22	22	22	22	22
$(OH)^{-*}$	0.17	0.72	0.41	0.42	0.28

*Note: * − values calculated based on compensation of charge. Analysis sum includes:*
1 − ThO_2 0.69 wt.% (corresponds to Th = 0.02 apfu);
3 − MgO 0.11 wt.% (corresponds to Mg = 0.03 apfu).

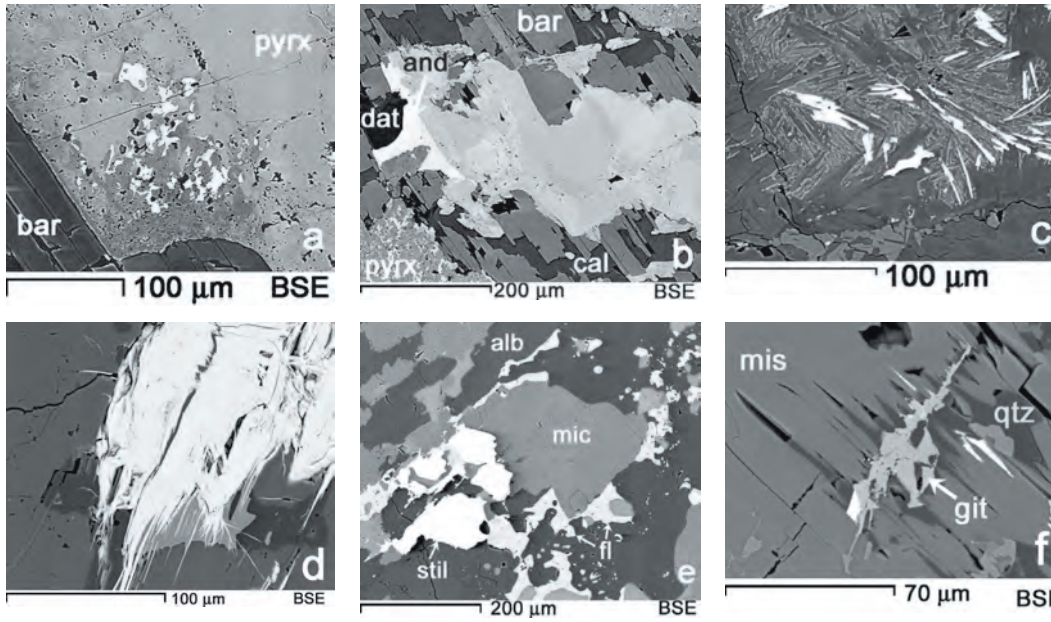

Fig. 7. Accessory minerals from baratovite-containing rocks of Hodzha-Achkan:
a — andradite — aegirine rim on the fringe of a coarse clinopyroxene grain (pyrx): bar — baratovite; light isolations — andradite; areas, enriched with aegirine component — darker in comparison with the less alkaline host pyroxene grains; black spots are cavities in the rock;
b — a zoned titanite crystal with baratovite (bar); pyrx — pyroxene grain near the aegirine — garnet rash; and — andradite; cal — calcite; dat — datolite;
c — ekanite: a deformed thin prismatic crystals in baratovite;
d — a mineral of hellandite group with Fe>> Ti: a thin — lamellar aggregate in baratovite;
e — stillwellite-(Ce): grains with microcline (mic), albite (alb), fluorite (fl);
f — gittinsite (git): isolated in miserite (mis); qtz — quartz; white grains — Ca-Ce-silicate.

it is a rock-forming mineral. It forms white to light gray board-like crystals up to 4 cm long. Its composition is close to stoichiometrical (Table 2, an. 6). *Calcite* in described rocks from Hodzha-Achkan, as well as in baratovite-containing quartz-albite-aegirine rocks from the Darai-Pioz (Reguir *et al.*, 1999), is enriched in strontium (SrO to 1.1 wt.%), similar to calcite in intrusive carbonatites. The accessory minerals (table 1) of the described rocks are similar to those in baratovite-containing quartz-albite-aegirine rocks from Darai-Pioz (Dusmatov *et al.*, 1975; Reguir *et al.*, 1999), although there are some differences. One of the most widespread accessory minerals not only at Hodzha-Achkan, but also in other alkaline massifs of a matchaisky complex, including the Darai-Pioz massif, is *titanite* (Omelyanenko, Sirotinina, 1959; Ilyinsky, 1970; Ifantopulo, 1975; Reguir *et al.*, 1999). The mineral forms wedge-shaped crystals to 5 mm in yellow-brown "flowers"; some segments demonstrate zonality and sectoriality and some of the zones are enriched in Sn, Nb, or *REE* (Fig. 7b, table 4, analysis 7).

The other widespread accessory minerals in the rocks described are *fluorbritholite-(Ce)* and the recently described *fluorcalciobritholite* (Pekov *et al.*, 2007) (Fig. 4d, table 4, an. 2). Their forms (to 300 microns) are often met in baratovite, miserite. Minerals of the britholite group are very rare at Darai-Pioz and were not seen in the baratovite rocks. *Garnets* (mainly of andradite composition) are another characteristic accessory mineral group in the Hodzha-Achkan rocks which were not found in baratovite-bearing rocks at Darai-Pioz. Except for isolated andradite in clinopyroxene external rims, as noted above, garnet forms isomeric apple-green grains (0.1—4 mm) in leucocratic varieties of rock (Table 2, an. 7). Sulfides often associated with garnet include *molybdenite*, *galena*, and *pyrite*.

Other accessory minerals at Hodzha-Achkan are *ekanite* (frequently seen) and *turkestanite* (more rare), the structures of which are similar (Fig. 7c, table 4, an. 4, 5). They form thin-prismatic (up to 0.2 mm long), often deformed, bent crystals and are intergrown with miserite and baratovite. Turkestanite, unlike

Table 4. **Chemical composition (wt.%) of the accessory minerals from baratovite − containing rocks of Hodzha-Achkan: stillwellite-(Ce) (1), fluorcalciobritholite (2), fluorapatite (3), turkestanite (4), ekanite (5), tadzhikite-(Ce) (6), titanite (7), gittinsite (8), bazirite (9)**

Component	1	2	3	4	5	6	7	8	9
SiO_2	21.63	19.06	0.75	54.63	53.85	24.86	29.94	39.49	37.45
TiO_2	0.00	0.00	0.00	0.00	0.00	3.86	33.24	0.39	0.35
ZrO_2	0.00	0.00	0.00	0.00	0.00	0.00	0.00	0.00	25.64
SnO_2	0.00	0.00	0.00	0.00	0.00	0.00	0.45	0.00	0.31
ThO_2	2.44	5.25	0.00	0.00	20.16	5.07	0.00	0.00	0.00
UO_2	0.00	0.00	0.00	0.00	10.08	0.99	0.00	0.00	0.00
P_2O_5	0.00	5.23	39.88	0.00	0.00	0.00	0.00	0.00	0.00
Nb_2O_5	0.00	0.00	0.00	0.00	0.00	0.00	1.68	2.07	0.00
B_2O_3	13.11*	n.d.	n.d.	n.d.	n.d.	14.31**	n.d.	n.d.	n.d.
Al_2O_3	0.00	0.00	0.00	0.22	0.12	0.44	1.48	0.00	0.00
Fe_2O_3	0.09	0.00	0.00	0.00	0.00	2.60	4.52	0.00	0.00
Y_2O_3	0.20	0.00	0.00	0.00	0.00	0.45	0.00	0.00	0.00
La_2O_3	23.35	14.62	0.69	0.00	0.00	6.25	0.65	0.00	0.00
Ce_2O_3	27.22	22.14	0.77	0.68	0.00	11.75	0.77	0.00	0.00
Pr_2O_3	1.16	1.84	0.00	0.00	0.00	0.85	0.00	0.00	0.00
Nd_2O_3	4.63	6.12	0.00	0.00	0.00	3.44	0.61	0.00	0.00
Sm_2O_3	0.19	0.00	0.00	0.00	0.00	0.16	0.00	0.00	0.00
Gd_2O_3	0.44	0.81	0.00	0.00	0.00	0.11	0.00	0.00	0.00
Tb_2O_3	0.50	0.71	0.00	0.00	0.00	0.00	0.00	0.00	0.00
SrO	0.38	0.48	0.90	0.00	0.00	0.00	0.00	0.00	0.00
CaO	1.66	19.29	53.41	9.18	12.48	20.78	27.51	18.71	0.23
MnO	0.10	0.00	0.00	0.00	0.00	0.00	0.00	0.49	0.00
BaO	0.00	0.00	0.00	0.00	0.00	0.00	0.00	0.00	33.22
PbO	0.19	0.00	0.00	0.59	0.74	0.04	0.00	0.00	0.00
K_2O	0.00	0.00	0.00	2.73	0.00	0.00	0.00	0.00	0.00
Na_2O	0.00	0.00	0.00	1.81	0.09	0.00	0.00	0.00	0.00
F	0.00	2.22	4.18	0.00	0.00	0.00	1.24	0.00	0.00
$-O=F_2$	0.00	0.00	−1.75	0.00	0.00	0.00	−0.58	0.00	0.00
Total	**98.67**	**99.58**	**100.58**	**99.00**	**95.45**	**96.16**	**101.74**	**99.99**	**97.20**

*Note: "n.d." means that the component was not detected. 1 − stillwellite-(Ce) ($Ce_{0.44}La_{0.38}Ca_{0.08}Mg_{0.07}Nd_{0.07}Th_{0.02}Pr_{0.02}$ $Gd_{0.01}$ $Tb_{0.01}Sr_{0.01})_{3.11}B_{0.99}Si_{0.95}O_5$, formula calculated on the basis of O = 5 apfu, analysis sum includes (wt.%): MgO 1.12, Tm_2O_3 0.24; * − B_2O_3 is measured using WDS with STE crystal, U = 10 κV, I = 70 nA; 2 − fluorcalciobritholite ($Ca_{2.64}Sr_{0.04}Ce_{1.04}$ $La_{0.69}Nd_{0.28}Pr_{0.09}Gd_{0.03}Tb_{0.03}Dy_{0.02}Th_{0.15}U_{0.05})_{5.02}$ $(SiO_4)_{2.43}(PO_4)_{0.57}(F_{0.89}OH_{0.38})$, formula calculated on the basis of Si + P = 3 apfu, analysis sum includes (wt.%): Dy_2O_3 0.24; H_2O 0.45 (calculated); 3 − fluorapatite-(CaF) $(Ca_{4.97}Sr_{0.05}Ce_{0.02}La_{0.02})_{5.06}(PO_4)_{2.93}$ $(SiO_4)_{0.07}F_{1.15}$, formula calculated on the basis of Si + P = 3 apfu; 4 − turkestanite $(Th_{0.92}U_{0.04}Ce_{0.04})_{1.00}(Ca_{1.43}Na_{0.51})_{1.94}(K_{0.51}$ $Pb_{0.02})_{0.53}(Si_{7.96}Al_{0.04})_{8.00}O_{19.93}$, formula calculated on the basis of Si+Al = 8 apfu; 5 − ekanite $(Th_{0.68}U_{0.33})_{1.01}(Ca_{1.98}Pb_{0.03}Na_{0.03})_{2.04}$ $(Si_{7.96}Al_{0.02})O_{20}$, formula calculated on the basis of O = 20 apfu; 6 − tadzhikite-(Ce) $Ca_2(Ca_{1.58}Y_{0.04}K_{0.04})_{1.66}(Ti_{0.47}Fe_{0.32}Al_{0.08})_{0.87}(Ce_{0.69}Pr_{0.05}$ $La_{0.37}Nd_{0.20}Sm_{0.01}Gd_{0.01}$ $Th_{0.19}U_{0.03})_{1.55}B_4Si_4O_{21.31}$, average of 3 analyses, formula calculated on the basis of Si = 4 apfu; ** B_2O_3 − calculated; 7 − titanite $(Ca_{0.96}Na_{0.01})_{0.97}(Ti_{0.82}Fe_{0.11}Al_{0.06}Nb_{0.02}Sn_{0.01}La_{0.01}Ce_{0.01}Nd_{0.01})_{1.05}Si_{0.98}O_{4.87}F_{0.13}$, formula calculated on the basis of cations sum = 3 apfu; 8 − gittinsite $(Ca_{1.00}Mn_{0.02})_{1.02}(Zr_{0.95}$ $Nb_{0.05}Ti_{0.01})_{1.01}Si_{1.97}O_{7.00}$, formula calculated on the basis of O = 7 apfu; 9 − bazirite $(Ba_{1.03}$ $Ca_{0.02})_{1.05}(Zr_{0.99}Sn_{0.01}Ti_{0.02})_{1.01}Si_{2.96}O$, formula calculated on the basis of O = 9 apfu.*

ekanite, is widespread at Darai-Pioz, where it is seen in many associations. In the Dzhilisuisky massif, neighboring Hodzha-Achkan, it is the main thorium concentrator (Ginzburg *et al.*, 1965; Pautov *et al.*, 1997; Reguir *et al.*, 1999). Among additional accessory minerals of the Hodzha-Achkan baratovite-bearing rocks are rare borosilicates of the hellandite group, including *tadzhikite-(Ce)* (Table 4, an. 6) and a poorly studied mineral, whose composition and X-ray powder data are close to those of tadzhikite, but with Fe>> Ti (Fig. 7d). These minerals are found as single grains, and as groups of flattened prismatic crystals up to 500 μm long as well as spherolites; their color is different shades of brown. It should be noted that at Darai-Pioz (which is the type locality for tadzhikite) (Efimov *et al.*, 1970), the mineral is a widespread accessory mineral, including an association with baratovite (Reguir *et al.*, 1999). Darai-Pioz's tadzhikite is not selective in *REE*, and two species of the tadzhikite subgroup — tadzhikite-(Y), and tadzhikite-(Ce) — are found there. Problems with crystal chemistry, rare earth distribution in the crystal structure of these minerals, and their nomenclature are discussed in a number of works (Chernitsova *et al.*, 1982; Hawthorne *et al.*, 1998; Reguir *et al.*, 1999; Oberti *et al.*, 1999; 2002). Unlike Darai-Pioz, at Hodzha-Achkan only cerium-dominant members of hellandite group are found. One additional accessory rare-earth borosilicate found in pyroxene-feldspar fenites with baratovite at Hodzha-Achkan is *stillwellite-(Ce),* which is found in the form of separate irregular grains (Fig. 7e; table 4, an. 1) up to 150 μm in size. Stillwellite-(Ce) is a very characteristic mineral of some Darai-Pioz rocks (Dusmatov *et al.*, 1963; Dusmatov 1964; 1971). On occasion it forms sharp crystals to several centimeters in diameter (Belakowski, 1991). In baratovite-containing quartz-albite-aegirine rocks at Darai-Pioz, stillwellite-(Ce) is described as crystals less than 50 μm in size, filling cracks and blebs in earlier formed minerals (Reguir *et al.*, 1999). Zirconium minerals in the baratovite rocks from the Hodzha-Achkan massif include gittinsite, bazirite, and zircon. *Gittinsite* is one of the late minerals; it is found in gap cracks in miserite crystals together with quartz (Fig. 7f, table 4, an. 1). At Darai-Pioz we found gittinsite only as a constituent part of eudialyte pseudomorphoses. At other locations where this mineral is found (the Kipava agpaitic complex in Canada (Ansell *et al.*, 1980) and the Khan-Bogdo rare-metal pegmatites in Mongolia (Tsareva *et al.*, 1993), it also occurs pseudomorphing minerals of the eudialyte group. *Bazirite* is a very rare mineral in baratovite-containing rocks of Hodzha-Achkan. It is found as single grains with hexagonal outlines to 50 μm (Table 4, an. 9). At Darai-Pioz, bazirite is seen with baratovite in association with titanite, filling in cracks in baratovite and aegirine (Reguir *et al.*, 1999), in pegmatites as a part of polymineral pseudomorphosis of eudialyte (Pautov, Khvorov, 1998), and in carbonatites with baratovite and aleksandrovite (Pautov *et al.*, 2010). *Zircon* is not a characteristic accessory mineral in baratovite-containing rocks of Hodzha-Achkan and Darai-Pioz; it is found in rare single grains. *Molybdenite* is the most typical sulfide mineral in the rocks of Hodzha-Achkan, with lamellar grains to 1.5 mm in diameter.

Baratovite description. Physical properties

Minerals of the baratovite-katayamalite series forms grains flattened on (001), thin lamellar grains, as a rule, without signs of crystallographic faces, sometimes forming fan-like aggregates, and more often random. The size of individual grains ranges from 0.02 mm to 2−3 cm, and the thickness of plates from 0.01 mm up to 1.0−1.5 mm (Fig. 4). The largest forms of baratovite are found in aegirine-feldspar rocks with miserite; baratovite in wollastonite rocks usually forms fine single grains (1−2 mm). Thin lamellar grains are transparent and colorless, while in larger grains pink coloring is observed. The luster is generally vitreous, although pearly on perfect cleavage planes. The mineral is very brittle, with perfect cleavage on (001). Two directions of cleavage are found, crossing the basal plane. In transparent sections in transmitted light baratovite is colorless, although cuts parallel to (001) have dark gray interference colors, and in slanted cuts abnormal indigo-blue interference colors are observed. The mineral is biaxial, optically positive, with 2V changeable from 70º to 90º, dispersion strong, $r > v$. The indices of refraction measured on the rotating spindle are as follows: $n_g = 1.674(2)$, $n_m = 1.671(3)$, $n_p = 1.666(3)$.

The microhardness of baratovite was measured in two sections (PMT-3 micro-durometer, calibrated on NaCl, loading 100 g): in the basal plane and perpendicular to it. Microhardness in the basal plane is VHN (kg/cm^2) = 615 (average of 10 measurements, dispersion 490−710). For cuts perpendicular

Table 5. **Cell dimensions of baratovite minerals group**

Name	*a*, Å	*b*, Å	*c*, Å	β, °	*V*, A^3	Location	Reference
Baratovite	16.93(1)	9.742(5)	20.92(2)	112.51(5)	3187(5)	Hodzha-Achkan, Kyrgyzstan	Our data (photomethod)
Baratovite	16.93(2)	9.733(5)	20.94(2)	112.49(7)	3187(7)	Hodzha-Achkan, Kyrgyzstan	Our data (diffractogramm)
Baratovite	16.90(2)	9.73(1)	20.91(2)	112.30	3179	Darai-Pioz, Tajikistan	Dusmatov *et al.,* 1975
Baratovite	16.953(5)	9.752(3)	20.916(6)	112.46(2)	3195.8	Darai-Pioz, Tajikistan	Sandomirsky *et al.,* 1976
Baratovite	16.941(3)	9.746(2)	20.907(3)	112.50(10)	3189.1	Darai-Pioz, Tajikistan	Menchetti, Sabelli, 1979
Katayamalite*	16.923(3)	9.721(2)	20.909(3)	112.40(10)	3180	Ivagi, Japan	Baur, Kassner, 1992
Aleksandrovite	17.01 (2)	9.751(6)	21.00(2)	112.45(8)	3219(7)	Darai-Pioz, Tajikistan	Pautov *et al.*, 2010

Note. * – α=*89.98(10);* γ=*89.94(10) (Baur, Kassner, 1992)*

to the basal plane poor 1st sort hardness anisotropy was observed (average of 17 measurements): across cleavage cracks VHN = 725 (dispersion 500–835); along cleavage cracks VHN = 620 (dispersion 495–700). The microhardness of baratovite from Darai-Pioz measured in similar conditions (on 10 measurements) is VHN = 615 both for sections (001) and cross-sections. The values found for microhardness of baratovite in both the Hodzha-Achkan samples and those from Darai-Pioz correspond to 5–6 on Moh's scale, which is higher than the original value of $3^1/_2$ noted in the original description of the mineral (Dusmatov *et al.*, 1975).

The mineral density measured in Clerichi solution by the equitation method for separate grains is $D_{meas.}$ = 2.92(2) g/cm^3. The calculated density based on the cell parameters, obtained from the X-ray space dimensions (Table 5) and average composition (Table 6, an. 1), is $D_{calc.}$ = 2.91 g/cm^3.

The baratovite-group minerals from Hodzha-Achkan, as well as baratovite from Darai-Pioz and katayamalite from Ivagi (Fig. 3), have a bright white-bluish fluorescence in short-wave UV-radiation. Heterogeneity of fluorescence intensity is observed among individual grains of baratovite. This effect is seen more intensely in the cathodoluminescence mode after excitation by an electron probe (Fig. 8). According to B.S. Gorobets and A.A. Rogozhin (2001), photoluminescence of Darai-Pioz baratovite is related to O*- and Fe^{+3}-luminescence centers. Subsequently, luminescence of baratovite from Darai-Pioz and katayamalite from Ivagi was studied by A. Sidike and coauthors (Sidike *et al.*, 2010), who related it to Ti–O_6 centers.

The IR spectrums of baratovite both from Darai-Pioz and Hodzha-Achkan are similar (Fig. 9), and have a strong double absorption band in the range of 900–1100 cm^{-1}, which is characteristic of ring silicates with sextuple rings of Si–O_4 – tetrahedrons, less strong bands in the range of 520–540 and 470–480 cm^{-1}, connected to ν_4 oscillation of Si–O_4, and an absorption band of 685–695 cm^{-1}, connected with ν_3 oscillation of Ti–O_6 (Povarennykh, 1979).

The chemical composition of baratovite

Only a few number of chemical analyses of baratovite and katayamalite have been published (Dusmatov *et al.*, 1975; Murakami *et al.*, 1983; Reguir *et al.*, 1999; Sidike *et al.*, 2010; Pautov *et al.*, 2010). Of these, the most complete is the analysis of katayamalite published by Nobihude Murakami with colleagues (1983). Other analyses do not provide data for all possible elemental components (i.e., there are no data for one or several of the following components: Li, F, OH). The most complete analysis of baratovite is found in the original description (Dusmatov *et al.*, 1975); it is calculated on the formula $KLi_2Ca_8Ti_2Si_{12}O_{37}F$, in contrast to $KLi_3Ca_7Ti_2[Si_6O_{18}]_2F_2$, as obtained from the structural analysis (Sandomirsky *et al.*, 1976; Menchetti, Sabelli, 1979). However, because data on water content are not shown in the first baratovite analysis (Dusmatov *et*

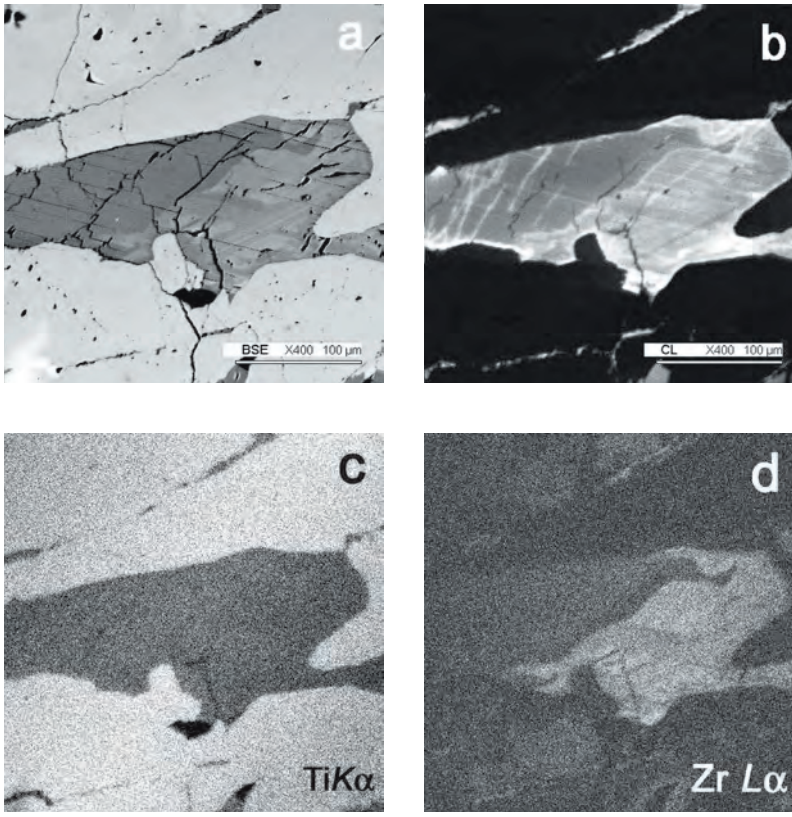

Fig. 8. Baratovite grain in titanite from miserite-aegirine-microcline rock, Hodzha-Achkan: a – BSE mode: grey – baratovite, light grey – titanite; b – cathodoluminescence mode; c, d – the X-ray image shows characteristic emission of TiKα (c) and ZrLα (d). The BSE image (fig. 8a) shows that there is complex inhomogeneity of the baratovite grain within the average atomic number; correlation with zirconium distribution (fig. 8d) is easily visible. The image in cathodoluminescence mode (fig. 8b) is much more complex: the general motif mirrors both the BSE image and the X-ray map of Zr distribution, but it is complicated by presence of areas, linear zones with a more intensive luminescence, possibly caused by deformations and an increased number of defects. Images are obtained by Camebax-microbeam with operating conditions: U = 15 kV, I = 20 nA.

al., 1975), and the fluorine content (Table 6, an. 5), after recalculation from the structural formula, is F = 0.79 apfu (which is less than half the number of additional anions in the formula), the legitimacy of katayamalite as a distinct mineral species has been questioned. Werner H. Baur and Dethard Kassner (1992), having reviewed the results of interpretation of the katayamalite structure $KLi_3Ca_7Ti_2[Si_6O_{18}]_2(OH)_2$, showed that this mineral, previously described as triclinic (Kato, Murakami, 1985), within experimental error can be well described by a monoclinic cell with space group *C*2/*c*. This is the same as baratovite, and baratovite's formula, considering the insufficient amount of fluorine according to the first analysis, should be written down as $KLi_3Ca_7(Ti,Zr)_2[Si_6O_{18}]_2(OH,F)_2$ (Baur, Kassner, 1992). Both the formulas $KLi_3Ca_7Ti_2[Si_6O_{18}]_2F_2$ (Clark, 1993; Anthony *et al.*, 1995; Minerals, 1996; Krivovichev, 2008), and $KLi_3Ca_7Ti_2[Si_6O_{18}]_2(OH,F)_2$ (Back, Mandarino, 2008) are published for baratovite in different handbooks. Based on our work, we consider that baratovite is the fluorine dominant mineral, while katayamalite is the hydroxyl dominant species. Since we were unable to find in the literature any analysis of baratovite in which fluorine and water were determined at the same time, except an electron probe analysis of the mineral (in which, along with other components, fluorine was defined), we attempted to obtain analytical data on the composition of the baratovite group minerals both from Hodzha-Achkan and from Darai-Pioz, including direct determination of F, OH, and Li.

Two samples of baratovite with large plates (one sample from Hodzha-Achkan and the other from Darai-Pioz, from miserite-bearing quartz-albite-aegirine rocks) were chosen for study. Pure material, free from visible inclusions, was separated under a binocular microscope in short-wave ultraviolet light. The weights of samples for determination of Li and Rb by ICP-OES method were 40–50 mg and by flame photometry 20 mg, for F determination by potentiometer method 20–30 mg, and for water determination by element analysis with chromatographic completion 2–7 mg (Table 6, analyses 1, 4). In the analyses of the mineral from Hodzha-Achkan, F (apfu) is

Table 6. **Chemical composition (wt.%) of baratovite and katayamalite from Hodzha-Achkan, Darai-Pioz and Ivagi**

Component	Hodzha-Achkan			Darai-Pioz				Ivagi		
	baratovite		katayamalite	baratovite			katayamalite	katayamalite		
	1	2	3	4	5	6	7	8	9	10
SiO_2	51.15	51.29	51.01	51.44	50.46	51.57	49.63	51.84	52.31	51.75
TiO_2	9.76	8.87	7.97	9.89	9.51	10.55	6.01	10.70	10.99	11.13
ZrO_2	1.74	2.22	3.71	1.18	2.28	0.90**	6.08	0.76	–	0.15**
SnO_2	0.46	1.01	0.87	0.87	–	>0.13**	2.04	0.17	0.00	0.06**
Nb_2O_5	0.04	0.00	0.23	0.18	0.72	>0.14**	0.00	0.04	–	0.07**
Al_2O_3	0.06	0.20	0.06	0.00	–	0.02	0.07	0.04	0.00	0.00
Fe_2O_3	0.39	0.60	0.44	0.46	0.50	0.31	0.29	0.23	0.29	0.26
CaO	27.48	26.72	26.72	27.12	30.36	27.36	26.67	27.00	28.25	28.58
MgO	0.03	0.00	0.00	0.03	–	0.00	0.00	0.01	0.00	0.01
MnO	0.11	0.00	0.00	0.10	0.50	0.34	0.15	0.20	0.22	0.07
K_2O	3.03	3.17	3.07	3.01	2.96	2.89	3.03	3.09	2.89	2.85
Na_2O	0.20	0.15	0.23	0.29	0.70	0.36	0.15	0.23	0.22	0.36
Li_2O	3.14	3.20*	3.17*	3.15	2.05	–	3.10*	3.22*	3.25	–
Rb_2O	0.12	n.d.	n.d.	–	–	0.075**	0.00	n.d.	–	0.023**
F	1.51	1.75	0.94	1.45	1.05	2.51	1.02	0.25	0.34	0.53
H_2O	0.61	0.46*	0.84*	0.68	–	–	0.76*	1.12*	1.21	–
$-O=F_2$	−0.63	−0.73	−0.39	−0.61	−0.44	–	−0.43	−0.11	−0.14	–
Total	**99.18**	**98.91**	**98.87**	**99.24**	**100.31**	–	**98.58**	**98.67**	**99.83**	–
Calculated on the basis of Si + Al = 12 apfu										
K^+	0.91	0.94	0.92	0.90	0.90	0.86	0.93	0.91	0.85	0.84
Na^+	0.09	0.07	0.10	0.13	0.32	0.16	0.07	0.10	0.10	0.16
Rb^+	0.02	–	–	–	–	–	–	–	–	–
Li^+	2.96	3.00	3.00	2.96	1.96	–	3.00	3.00	3.00	–
Ca^{+2}	6.90	6.67	6.73	6.78	7.74	6.82	6.90	6.69	6.94	7.10
Mg^{+2}	0.01	0.00	0.00	0.01	0.00	0.00	0.00	0.00	0.00	0.00
Mn^{+2}	0.02	0.00	0.00	0.02	0.02	0.07	0.03	0.04	0.04	0.01
Ti^{+4}	1.72	1.55	1.41	1.73	1.71	1.85	1.09	1.86	1.90	1.94
Zr^{+4}	0.20	0.25	0.42	0.13	0.26	–	0.72	0.09	–	–
Sn^{+4}	0.04	0.09	0.08	0.08	–	–	0.20	0.02	–	–
Nb^{+5}	0.00	0.00	0.02	0.02	0.08	–	0.00	0	–	–
Fe^{+3}	0.07	0.11	0.08	0.08	0.09	0.05	0.05	0.04	0.05	0.05
Al^{+3}	0.02	0.05	0.02	–	–	0.00	0.02	0.01	–	0.00
Si^{+4}	11.98	11.95	11.98	12.00	12.00	12.00	11.98	11.99	12.00	12.00
F^-	1.12	1.29	0.70	1.07	0.79	1.84	0.77	0.18	0.25	0.39
OH^-	0.95	0.71	1.30	1.06	–	–	1.23	1.72	1.85	–
O^{-2}	35.92	35.64	35.72	35.79	37.23	–	36.02	35.78	35.78	–

Note: «–» means, that data for a component are not provided.

** – H_2O and Li_2O calculated on basis of (F + OH) = 2.00 apfu, Li = 3.00 apfu. 1 – average of 47 electron-microprobe analyses, instead: Li_2O (average from two analyses obtained both by ICP OES and flame photometry methods); Rb_2O (flame photometry); F (potentiometry); H_2O (CHN-analysis with chromatographic completion, average of 3 determinations); 2 – electron-microprobe analysis (with maximum F amount); 3 – electron-microprobe analysis (with maximum $H_2O_{calc.}$ amount); 4 – average of 11 electron-microprobe analyses (3 analyses – WDS JCXA 733, 8 analyses – EDS ISIS, CamScan-4D) instead: Li_2O (average from two analyses obtained both by ICP OES and flame photometry methods); F (potentiometry); H_2O (CHN-analysis with chromatographical completion, average of 2 determinations); 5 – «wet chemistry», analyst A.V. Bykova (Dusmatov et al., 1975); 6 – electron-microprobe analyses, ** – calculated on oxides from ICP-MS data. Besides, (ppm): Zn 240, Sr 903, Cs 168, Ba 4410, Hf 294 (data with amounts >100 ppm are given) (Sidike et al., 2010); 7 – electron-microprobe analyses (Pautov et al., 2010); 8 – electron-microprobe analyses (WDS); 9 – electron-microprobe analyses, Li_2O – flame photometry; H_2O – gravimetry; F – potentiometry) (Murakami et al., 1983); 10 – electron-microprobe analyses, ** – calculated on oxides from ICP-MS data. Besides, (ppm): Zn 340, Sr 754, Ba 2570, Ta 187 (data with amounts >100 ppm are given)(Sidike et al., 2010).*

Table 7. **Representative electron probe analyses (wt.%) data sampling for baratovite and katayamalite from the Hodzha-Achkan massif**

Component	Baratovite							Katayamalite							
	1	2	3	4	5	6	7	8	9	10	11	12	13	14	15
SiO_2	51.75	52.08	50.85	50.72	50.93	52.00	50.83	51.48	51.80	51.47	51.77	51.32	51.79	51.48	51.76
TiO_2	8.71	10.13	9.62	9.93	10.14	10.01	9.87	9.77	9.96	9.56	10.27	10.14	9.88	7.83	9.43
ZrO_2	2.25	1.12	1.38	1.27	1.28	1.61	1.97	1.65	1.22	1.44	1.50	1.80	1.22	3.68	1.78
SnO_2	1.01	0.00	0.64	0.85	0.71	0.72	0.00	0.13	0.74	0.13	0.67	0.74	0.76	0.87	1.29
Nb_2O_5	0.00	0.00	0.00	0.00	0.00	0.00	0.00	0.03	0.00	0.08	0.44	0.00	0.00	0.00	0.00
Al_2O_3	0.18	0.19	0.00	0.11	0.00	0.00	0.00	0.07	0.00	0.07	0.00	0.00	0.00	0.00	0.10
Fe_2O_3	0.60	0.44	0.36	0.22	0.23	0.60	0.39	0.43	0.39	0.43	0.76	0.73	0.35	0.44	0.41
CaO	26.73	28.54	27.86	27.78	27.58	28.09	27.73	27.15	28.13	27.16	28.25	27.91	28.12	26.73	26.85
MgO	0.00	0.00	0.00	0.10	0.11	0.00	0.00	0.05	0.00	0.02	0.00	0.00	0.00	0.00	0.00
MnO	0.00	0.27	0.00	0.00	0.00	0.00	0.22	0.15	0.00	0.20	0.19	0.00	0.00	0.00	0.00
K_2O	3.17	2.83	3.20	2.90	2.85	2.95	2.95	3.03	3.14	3.06	2.96	3.13	3.14	3.07	3.03
Na_2O	0.15	0.38	0.23	0.26	0.27	0.33	0.31	0.21	0.19	0.19	0.21	0.29	0.20	0.23	0.14
Li_2O^*	3.17	3.10	3.12	3.13	3.14	3.08	3.13	3.18	3.09	3.20	3.01	3.02	3.08	3.16	3.16
F	1.76	1.64	1.56	1.53	1.41	1.47	1.36	1.25	1.25	1.24	1.22	1.06	1.07	0.98	0.97
H_2O^*	0.47	0.53	0.54	0.55	0.61	0.61	0.63	0.70	0.70	0.71	0.72	0.79	0.79	0.82	0.83
$-O=F_2$	-0.74	-0.69	-0.66	-0.64	-0.59	-0.62	-0.57	-0.53	-0.53	-0.52	-0.51	-0.44	-0.45	-0.41	-0.41
Total	99.21	100.56	98.70	98.71	98.67	100.85	98.82	98.75	100.08	98.44	101.46	100.49	99.95	98.88	99.34
Calculated on the basis of Si + Al = 12 apfu															
K^{+1}	0.93	0.83	0.96	0.87	0.86	0.87	0.89	0.90	0.93	0.92	0.88	0.93	0.93	0.91	0.89
Na^{+1}	0.07	0.17	0.11	0.12	0.12	0.15	0.14	0.09	0.09	0.09	0.09	0.13	0.09	0.10	0.06
Li^{+1}	3.00	3.00	3.00	3.00	3.00	3.00	3.00	3.00	3.00	3.00	3.00	3.00	3.00	3.00	3.00
Ca^{+2}	6.61	7.02	7.04	7.02	6.96	6.95	7.01	6.77	6.98	6.77	7.02	6.99	6.98	6.68	6.65
Mg^{+2}	0.00	0.00	0.00	0.04	0.04	0.00	0.00	0.02	0.00	0.01	0.00	0.00	0.00	0.00	0.00
Mn^{+2}	0.00	0.05	0.00	0.00	0.00	0.00	0.04	0.03	0.00	0.04	0.04	0.00	0.00	0.00	0.00
Ti^{+4}	1.51	1.75	1.71	1.76	1.80	1.74	1.75	1.71	1.74	1.67	1.79	1.78	1.72	1.37	1.64
Zr^{+4}	0.25	0.13	0.16	0.15	0.15	0.18	0.23	0.19	0.14	0.16	0.17	0.21	0.14	0.42	0.20
Sn + 4	0.09	0.00	0.06	0.08	0.07	0.07	0.00	0.01	0.07	0.01	0.06	0.07	0.07	0.08	0.12
Nb^{+5}	0.00	0.00	0.00	0.00	0.00	0.00	0.00	0.00	0.00	0.01	0.05	0.00	0.00	0.00	0.00
Fe^{+3}	0.10	0.08	0.06	0.04	0.04	0.10	0.07	0.08	0.07	0.08	0.13	0.13	0.06	0.08	0.07
Al^{+3}	0.05	0.05	0.00	0.03	0.00	0.00	0.00	0.02	0.00	0.02	0.00	0.00	0.00	0.00	0.03
Si^{+4}	11.95	11.95	12.00	11.97	12.00	12.00	12.00	11.98	12.00	11.98	12.00	12.00	12.00	12.00	11.97
F^{-1}	1.29	1.19	1.16	1.14	1.05	1.07	1.02	0.92	0.92	0.91	0.89	1.22	1.22	0.72	0.71
OH^{-1}	0.71	0.81	0.84	0.86	0.95	0.93	0.98	1.08	1.08	1.09	1.11	0.78	0.78	1.28	1.29
O^{-2}	35.43	35.92	36.02	36.08	36.09	36.04	36.13	35.75	35.99	35.64	36.4	36.4	36.02	35.54	35.63

*Notes: * — H_2O and Li_2O are calculated on the basis of (F + OH) = 2.00 apfu, Li = 3.00 apfu.*

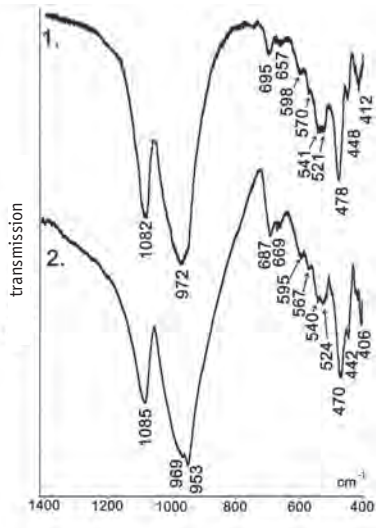

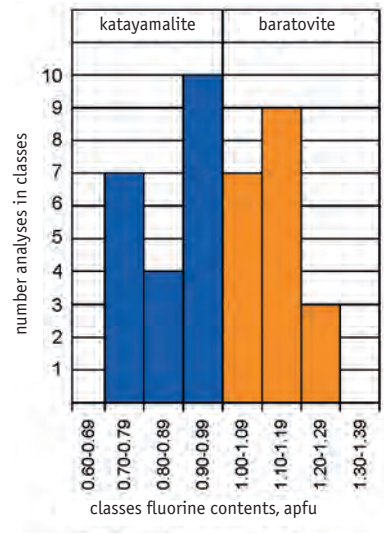

Fig. 9. Baratovite IR spectra: 1 — Hodzha-Achkan (operating conditions — microtablet with KBr, Specord-75IR); 2 — Darai-Pioz (operating conditions — tablet with KBr, Avatar 370 FT-IR Fourier spectrometer).

Fig. 10. A histogram of fluorine distribution in the baratovite-katayamalite mineral series from the Hodzha-Achkan massif (based on 40 analyses).

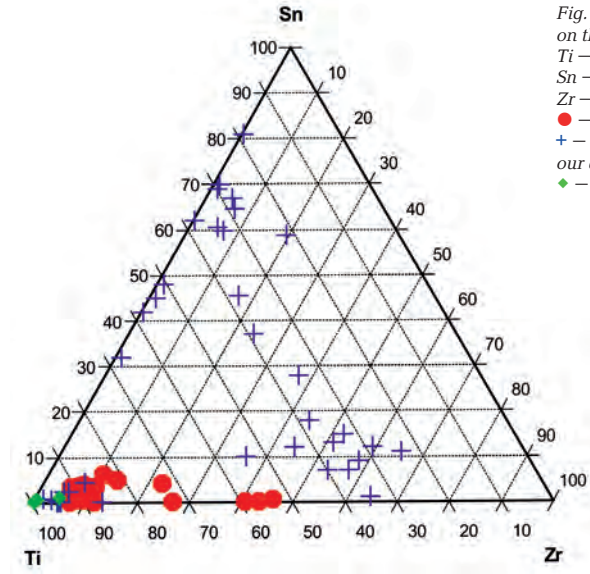

Fig. 11. Compositions (mol. %) of the baratovite mineral group on the ternary chart of end members:
Ti — baratovite and katayamalite;
Sn — aleksandrovite;
Zr — zirconium analog of baratovite:
● — Hodzha-Achkan (by results of 48 electron probe analyses);
+ — Darai-Pioz (Dusmatov et al., 1975; Reguir et al., 1999 and our data);
◆ — Ivagi (Murakami et al., 1983; our data).

slightly more prevalent than OH, while this ratio is close to 1:1 for the mineral from Darai-Pioz. Because different parts of crystals, which can differ in F/OH ratio, are mixed in these samples, these analyses represent an average of the material from each locality. Localized electron probe analyses show that F amounts in the baratovite group minerals of Hodzha-Achkan and Darai-Pioz massifs are changeable and correspond to both hydroxyl- and fluorine-dominant phases. A histogram of F distribution, based on electron probe analysis, for minerals of baratovite group from Hodzha-Achkan is shown in figure 10, which also shows that most of the analyses are approximately in the middle of the baratovite-katayamalite series.

The baratovite from Hodzha-Achkan, unlike katayamalite from Ivagi, is slightly enriched in tin and zirconium, making it similar to baratovite from Darai-Pioz, where tin and zirconium are concentrated up to a tin baratovite analog (aleksandrovite) and an unnamed Zr-analog of baratovite (Fig. 11; tables 6, 7). Occupation of the *M*2 octahedral position of baratovite with zirconium is probably the result of crystallization of the mineral from high-alkaline conditions. As

Table 8. **X-ray powder diffraction data on baratovite from the Hodzha-Achkan massif**

Photo-method		Diffrac-togram		Calculated data					Photo-method		Diffrac-togram		Calculated data				
I	*d*, Å	*I*	*d*, Å	*I*	*d*, Å	*h*	*k*	*l*	*I*	*d*, Å	*I*	*d*, Å	*I*	*d*, Å	*h*	k	l
		1	9.70	3	9.663	0	0	2	20	2.106	2	2.108	10	2.107	4	2	5
20	8.34	1	8.31	6	8.269	1	1	0			2	2.095	4	2.101	-2	4	5
		2	7.70	6	7.686	-2	0	2	10	2.091			2	2.083	6	2	2
30	7.04	2	7.03	13	7.024	-1	1	2	20	2.082			10	2.079	7	1	1
10	5.74	4	5.74	12	5.735	1	1	2	10	2.078			4	2.077	3	1	7
		2	5.19	3	5.185	2	0	2	10	2.070			3	2.071	-4	2	9
		1	5.08	4	5.069	-2	0	4	20	2.043			5	2.043	-5	3	7
		2	4.83	2	4.832	0	0	4	< 10	2.027			4	2.029	5	1	5
20	4.606	4	4.599	8	4.597	3	1	0	40	2.006			14 6	2.009 2.008	1 2	3 4	7 4
20	4.354	3	4.352	8	4.350	0	2	2	10w	1.997			4	2.000	-1	3	8
10	4.266			32	4.231	-4	0	2	20	1.981			14	1.985	-5	1	10
100	4.229	23	4.234	38	4.222	-2	2	1	10	1.943			12 3	1.944 1.943	4 -7	2 3	6 3
10	4.169			8	4.166	3	1	1	10w	1.932	3	1.932	11	1.933	0	0	10
10	4.138	7	4.139	16	4.135	2	2	0	10w	1.911			2	1.911	-4	2	8
		3	4.120	14	4.114	-2	2	2	20	1.883			4	1.888	-2	4	7
90	4.088	13	4.092	43	4.090	-3	1	4	30w	1.872			6	1.863	7	1	3
80	3.889	16	3.889	43	3.885	0	2	3	20w	1.855			7	1.853	1	3	8
30	3.852	7	3.849	1 9	3.852 3.846	-2 1	2 1	3 4	10	1.849			2	1.848	6	2	4
		1	3.810	1	3.810	-1	1	5	30	1.845			26	1.846	-9	1	4
100	**3.696**	**29**	**3.697**	81	3.695	3	1	2	40	1.842	8	1.841	15 26	1.842 1.840	-9 -3	1 5	5 1
40	3.620	8	**3.621**	22	3.621	-3	1	5	10	1.838			26 24	1.839 1.838	-3 -6	5 4	2 2
10	3.555	4	3.552	2	3.550	2	2	2	10	1.832			15 20	1.834 1.832	-9 -6	1 4	3 4
10	3.513	3	3.519	4	3.512	-2	2	4	30w	1.823			11 4 5	1.825 1.822 1.822	3 -9 -7	5 1 1	0 6 10
20	3.482	4	3.486	6	3.485	-2	0	6	< 10	1.795			5	1.797	4	2	7
30	**3.433**	**19**	**3.432**	43	3.430	0	2	4	< 10	1.789			4	1.791	2	4	6
10	3.359	3	3.391						20	1.776			8	1.779	3	3	7
30	**3.260**	**9**	**3.263**	18	3.258	3	1	3	10w	1.762			2	1.763	-1	5	5
40	3.224			12	3.221	4	0	2	10	1.748			2 1	1.749 1.749	8 -2	2 2	1 11
100	**3.222**	**100**	**3.223**	100	3.221	0	0	6	20	1.742			5	1.743	-3	5	5
10	3.209			26	3.198	2	2	3	20	1.737	2	1.736	7 8	1.739 1.735	-9 6	1 2	8 5
90	**3.193**	**47**	**3.194**	94	3.192	-3	1	6	10	1.731			9	1.731	6	4	1
20	3.167	6	3.167	8	3.161	-4	2	1	10	1.716			12	1.714	-6	4	7
40	3.156			14	3.161	-2	2	5	40	1.712	2	1.713	11	1.711	9	1	0
20	3.147	11	3.149	23	3.147	-4	0	6	40	1.697			8	1.697	3	5	3
10	3.139			2	3.143	-4	2	3	20	1.687			6	1.686	-3	5	6
< 10	3.125	1	3.120	7	3.120	-5	1	1	10	1.683			4	1.682	-9	1	9
30w	3.098	**25**	**3.095**	35	3.099	1	3	1	10	1.679			1	1.676	-2	4	9
30w	3.088			48	3.087	-5	1	4	10w	1.672			2	1.674	6	4	2
30	3.051	43	3.044	75	3.049	4	2	0	10w	1.665			5	1.667	4	2	8
30	3.030	2	2.999	57	3.028	0	2	5	10	1.636			11	1.640	-3	3	11
10	2.980			5	2.978	5	1	0	20	1.629			8	1.629	6	2	6
90	**2.953**	**11**	**2.953**	99	2.953	1	3	2	20w	1.608	1	1.615	15	1.611	0	4	9

Table 8. **Continue**

Photo-method		Diffrac-togram		Calculated data					Photo-method		Diffrac-togram		Calculated data				
I	*d*, Å	*I*	*d*, Å	*I*	*d*, Å	*h*	*k*	*l*	*I*	*d*, Å	*I*	*d*, Å	*I*	*d*, Å	*h*	k	l
20	2.942			3	2.944	-1	3	3	10	1.603			2	1.604	8	2	3
														1.601	0	6	2
80	**2.932**	**9**	**2.932**	92	2.932	-5	1	5	10	1.593			9	1.595	-6	2	12
				78	2.882	4	2	1					2	1.589	-8	4	5
80	2.882	14	2.883	51	2.880	3	1	4	10w	1.588			3	1.589	-2	6	2
														1.588	-1	3	11
< 10	2.863			11	2.868	2	2	4	10w	1.579			3	1.580	-5	1	13
													2	1.572	-2	6	3
10	2.837	3	2.833	7	2.834	-2	2	6	10	1.572			2	1.571	-8	4	6
													1	1.571	3	5	5
10	2.807	2	2.807	10	2.809	-3	3	1	10	1.569			4	1.570	-9	3	1
													3	1.560	-3	5	8
		2	2.800	4	2.801	-6	0	2	10	1.558			3	1.560	-10	2	2
													3	1.551	4	2	9
20	2.795			13	2.794	5	1	1	10	1.551			1	1.550	1	5	7
													6	1.544	6	4	4
60	2.767	4	2.766	37	2.767	1	3	3	20	1.543			5	1.544	-8	4	7
20	2.757			18	2.756	-1	3	4	10	1.538			7	1.539	0	6	4
50	**2.740**	**3**	**2.742**	31	2.741	-5	1	6	10	1.531			8	1.531	6	2	7
													4	1.524	-5	3	12
40	**2.686**	**3**	**2.688**	19	2.687	4	2	2	30	1.523			5	1.522	-6	4	10
10	2.655			3	2.655	3	3	1	10	1.515			9	1.518	9	1	3
													5	1.512	-2	6	5
20	2.641	**3**	**2.643**	13	2.643	-4	2	6	30	1.510			8	1.512	-9	3	9
10	2.618			2	2.607	6	0	0	20	1.496			3	1.495	0	6	5
30	2.592			4	2.593	4	0	4	10	1.487			7	1.488	9	3	1
20	2.567			8	2.566	1	3	4	10	1.482			6	1.484	-1	3	12
													4	1.473	-4	6	5
10	2.552			7	2.555	-1	3	5	10	1.471			1	1.472	-2	6	6
20	2.535			8	2.538	-5	1	7	10	1.463			4	1.465	7	1	7
20	2.495			2	2.496	-3	3	5	20	1.419			4	1.421	-8	4	10
													7	1.381	3	1	12
10	2.485			10	2.484	4	2	3	10	1.378			6	1.380	0	0	14
													3	1.378	6	6	0
30	2.441			6	2.441	-4	2	7	10	1.370			3	1.371	-6	6	6
													6	1.354	-12	2	5
< 10	2.431			5	2.428	-6	2	2	10	1.353			2	1.353	-9	5	4
													2	1.353	-5	3	14
				4		-6	2	4					6	1.351	-3	7	1
40	2.412	5	2.416	13	2.416	0	4	1	10	1.349			6	1.350	-3	7	2
				17		0	0	8					6	1.348	-9	5	3
10	2.398			7	2.392	5	1	3	10	1.342			5	1.343	-9	5	6
													3	1.343	-3	7	
30	2.366			5	2.367	3	3	3	20	1.336			5	1.338	-12	2	8
				14		1	3	5									
10	2.354			5	2.353	-1	3	6	10	1.331			4	1.332	3	7	1
													2	1.332	-12	2	3
30	2.340			4	2.339	-7	1	4	20	1.326			4	1.327	6	6	2
40	2.339	3	2.339	12	2.339	-5	1	8	10	1.315			5	1.318	5	1	11
30w	2.285	**2**	**2.287**	9	2.289	4	2	4	20w	1.275			2	1.277	-2	6	10
													3	1.181	7	7	0
20w	2.181	2	2.182	9	2.184	-3	3	7	10w	1.181			1		0	8	4
													3	1.169	-2	8	5
< 10	2.153			9	2.154	-5	1	9	10w	1.168			4	1.166	6	4	10
< 10	2.141			2	2.145	-5	3	6	10w	1.143			6	1.145	7	7	2

Note. Photomethod: Huber 621 Guinier camera with a quartz monochromator; CuKα_1 radiation; quartz as the internal standard. Diffractogram: DRON-2.0, CuKα radiation, Ni — filter, quartz as the internal standard. Indexes and intensities for calculated data column are taken from www.rruff.info. Lines used for calculation of cell dimensions (tab. 5) are highlighted in bold type, w — widened line.

experimental work shows, in this case introducing zirconium into structures with coordination [6] (for example, in pyroxene, or amphibole structures), is preferable to formation of phases with a higher coordination of [7] or [8] (Jones, Peckett, 1980; Linthout, 1984; Duggan, 1988, Farges *et al.*, 1994; Piilonen *et al.*, 1998). This may explain the extreme rarity of zircon in these rocks. The problems of zirconium genetic crystal chemistry have been considered in a number of publications in detail (Pyatenko *et al.*, 1999; Pekov, 2005). The entry of tin into minerals of the baratovite, titanite, milarite and astrophyllite groups shows that tin behavior in high-alkaline systems in many respects is similar to that of titanium and zirconium.

X–ray powder diffraction data

Since X-ray powder data published in literature for baratovite (Dusmatov *et al.*, 1975) and katayamalite (Murakami *et al.*, 1983) are much poorer in reflections than calculated data, we have obtained not only the diffractogram (which can be complicated by almost inevitable texturing of material), but also powder data by photomethod in the Guinier camera (table 8). The X-ray powder diffraction data were obtained from Hodzha-Achkan samples from which material for wet chemistry determination of fluorine, water and rare alkalis was extracted. Material for powder data by Guinier method was extracted from the sample of baratovite in miserite-feldspar-aegirine rock (operating number 11HA_58). The parameters of cells calculated for both powder data, and also for baratovite, katayamalite and aleksandrovite taken from references, are shown in table 5.

Conclusions

(1) Very rare minerals of the baratovite-katayamalite series are found in fenite rocks of the Hodzha-Achkan massif (Kyrgyzstan). The find of baratovite is most likely the second, and that of katayamalite the third in the world.

(2) A complete wet chemical analysis of baratovite, including determination of Li_2O, H_2O, and F was performed for the first time. New data for minerals of the baratovite group were obtained, including more complete powder data and the mineral microhardness, which corresponds to 5–6 on the Moh's scale, a value higher than recorded in the previous literature.

(3) Baratovite and katayamalite, both at Darai-Pioz, and Hodzha-Achkan, has been found in pyroxene-feldspar fenites (according to fenite's classification of (Bardina, Popov, 1993)). In these rocks the minerals miserite (to 5.5 wt.% REE_2O_3), turkestanite, bazirite, and the rare boronsilicates-tadzhikite and stillwellite-(Ce) occur. However there are also differences between the fenites of Hodzha-Achkan and Darai-Pioz. First, the former is a little less alkaline, and, perhaps, of higher-temperature origin, than similar rocks at Darai-Pioz. Clinopyroxene from the Hodzha-Achkan massif fenites is poorer in aegirine in contrast to Darai-Pioz, and, especially, to Ivagi syenites. Unlike Darai-Pioz, in the Hodzha-Achkan fenites a garnet (andradite) occurs. If we compare thorium silicates, at Hodzha-Achkan ekanite, which is non-alkaline, is typical, whereas at Darai-Pioz its place is taken by alkaline turkestanite. The most important *REE* mineral is britholite, absent in Darai-Pioz's fenites. We have not excluded the possibility that katayamalite-containing rocks of Ivagi (Murakami *et al.*, 1983) are not syenites, but that they are high-alkaline fenites; yet we do not have enough of the actual material to confirm this.

(4) Baratovite and katayamalite in miserite-containing fenites of Darai-Pioz and of Hodzha-Achkan are the only lithium minerals, and are important concentrators of zirconium and tin.

(5) We believe, in contrast to Reguir and coauthors (Reguir *et al.*, 1999), that the origin of the baratovite-containing rocks of Hodzha-Achkan and Darai-Pioz is not a unique combination of several processes occurring at different times with different sources of substrate, but is a single complex process, with a common source of fenitization solutions. It is possible that carbonatites (Mayorov, Gavrilin, 1971), or syenite-carbonatites (Fayziyev *et al.*, 2010) were such sources.

(6) The Darai-Pioz mineralization, which has been represented in the past as unique, is duplicated to some extent in massifs of a matchaisky complex (and may be duplicated again in other occurrences). Our work on the baratovite-containing fenite rocks of the Hodzha-Achkan massif shows this clearly.

Acknowledgements

The authors are grateful for the help in the organization or for participation in field work on the Hodzha-Achkan and Darai-Pioz massifs to P.V. Khvorov, V.A. Muftakhov, T.K. Ber-

kelyev, A.R. Faiziev, V.S. Gursky, V.V. Smirnov, K.E. Ibrayev, R.U. Sobirova, I.N. Solodkova, L.L. Berezhnaya; for discussions and valuable advice to E.M. Spiridonov, I.V. Pekov, Yu.D. Gritsenko, P. M. Kartashov; to Kotaro Watanabe for the katayamalite sample, provided for study from its type locality (Ivagi, Japan) and also to Dr. M. Feinglos for english text editing.

References

Agakhanov A.A., Pautov L.A., Karpenko V.Yu, Bekenova G.K., Uvarova Yu.A. Orlovite $KLi_2TiSi_4O_{11}F$ — a new mineral from the mica group from Darai-Pioz massif (Tadzhikistan) // New data on minerals. **2011**. Vol. 46. P. 13—19 (in Russian).

Ansell H.G., Roberts A.C., Plant A.G., Sturman B.D. Gittinsite, a new calcium zirconium silicate from the Kipawa agpaitic syenite complex, Quebec // Canad. Mineral. **1980**. Vol. 18. N 2. P. 201—203.

Anthony J.W., Bideaux R.A., Bladh K.W., Nichols M.C. Handbook of Mineralogy. Vol. II. Silica, Silicates. Part 1—2. Tucson: Mineral Data Publishing. **1995**. 904 p.

Back M.E., Mandarino J.F. Fleisher's Glossary of mineral species 2008. Tucson: The Mineralogical Record Inc. **2008**. 345 p.

Bardina N.Yu., Popov V.S. Fenites: a systematics, conditions of origin and value for a crust magmatical forming // ZVMO. **1994**. Vol. 123. № 6. P 1—19 (in Russian).

Baur W.H., Kassner D. Katayamalite and baratovite are structurally identical // Eur. J. Mineral. **1992**. Vol. 4. P. 839—841.

Belakowski D.I. Die seltenen Mineralien von Darai-Pioz in Hochgebirge Tadshikistans // Lapis. **1991**. 16. № 12. 42—48.

Berry L. G., Lin H.-c., Davis G. C. A new occurrence of miserite from the Kipawa Lake area, Temiscamingue Co., Quebec // Canad. Mineral. **1971**. Vol. 11. N 2. P. 569.

Chernitsova N.M., Pudovkin Z.V., Pyatenko Yu.A. About crystal structure of tadzhikite $(Ca,TR)_4(Y,TR)_2(Ti,Fe,Al)(O,OH)_2[Si_4B_4O_{22}]$ // Dokl. AN SSSR. **1982**. Vol. 264. N 2. P. 342—344 (in Russian).

Clark A.M. Hey's mineral index. London: Chapman and Hall. **1993**. 852 p.

Dawson J.B., Hill P.G. Mineral chemistry of a peralkaline combeite lamprophyllite nephelinite from Oldoinyo Lengai, Tanzania // Mineral. Magaz. **1998**. Vol. 62. N 2. P. 179—196.

Dorfman M.D., Timofeev V.D. To petrography of the Hodzhaachkan alkaline massif // Trudy Petrogr. Inst. **1939**. Vol. 14. P. 153—195 (in Russian).

Duggan M.B. Zirconium-rich sodic pyroxenes in felsic volcanics from the Warrumbungle Volcano, Central New South Wales, Australia // Mineral. Magaz. **1988**. Vol. 52. P. 491—496.

Dusmatov V.D. About the first find of a stillwellite in the USSR // Dokl. AN Tadjik. SSR. **1964**. T. 7. № 2. P. 33—34 (in Russian).

Dusmatov V.D. Mineralogy of the Darai-Pioz alkaline massif (Southern Tien Shan). Candidate's dissertation. M.: IMGRE. **1971**. 171 p. (in Russian)

Dusmatov V.D., Efimov A.F., Semenov E.I. The first finds of a stillwellite in the USSR // Dokl. AN USSR. **1963**. Vol. 153. № 4. P. 913—915 (in Russian).

Dusmatov V.D., Semenov E.I., Khomyakov A.P., Bykova A.V., Dzhafarov N.H. Baratovite — a new mineral // ZVMO. **1975**. Vol. 104. № 5. P. 580—582 (in Russian).

Efimov A.F., Dusmatov V.D., Alkhazov Yu.A., Pudovkina Z.G., Kazakova M.E. Tadzhikite — a new boronsilicate of rare earthes from the hellandite group // Dokl. AN SSSR. **1970**. Vol. 195. № 5. P. 1190—1193 (in Russian).

Enikeeva L.N., Pomazkov Ya.K., Akkermantsev S.M. Mizerite from gabbroids of the Hodzhaachkan massif (Kirgizia) // Zap. Uzbek. otd. VMO. **1987**. Vol. 40. P. 64—66 (in Russian).

Farges F., Brown G.E., Velde D. Strucrural environment of Zr in two inosilicates from Cameroon: mineralogical and geochemical implications // Amer. Mineral. **1994**. Vol. 79. N 9—10. P. 838—847.

Fayziyev A.R., Gafurov F.G., Sharipov B.N. Carbonatites of the Darai-Piyoz massif of alkaline rocks (Central Tajikistan) and features of their composition // Geokhimiya. **2010**. № 11. P. 1154—1168 (in Russian).

Geological map of Kirgiz SSR. Scale 1:500 000 (under the ed. of S.A. Ingemberdiev). Ministry of geol. USSR; Acad. Sci Kirg. SSR. **1980**.

Geological map of Tadjik SSR and adjacent territories. Scale 1:500 000 (under the ed. of N.G. Vlasov and Yu.A. Djakov). Ministry of geol. USSR. **1984**.

Ginzburg I.V., Semenov E.I., Leonova L.L., Sidorenko G.A., Dusmatov V.D. A crystalline ekanite from Central Asia, rich with alkalis // Trudy Mineral. Muzeya (Transac. Miner. Museum). Acad. Nauk SSSR. **1965**. Vol. 16. P. 57—72(in Russian).

Gorobets B.S., Rogozhin A.A. Luminescent spectrums of minerals. Handbook. M.: VIMS (All-Union Inst. Min. Raw mater.). **2001**. 312 p. (in Russian)

Hawthorne F.C., Cooper M.A., Taylor M.C. Refinement of the crystal structure of tadzhikite // Canad. Mineral. **1998**. Vol. 36. N. 2. P. 817–822.

Ifantopulo T.N. Mineralogical-geochemical features of alkaline rocks of Central Turkestano-Alay. M: Nedra. **1975**. 129 p. (in Russian).

Ilyinsky G.A. Mineralogy of alkaline intrusions of the Turkestano-Alay. L.: LGU (Leningrad State Univ. **1970**. 166 p. (in Russian).

Jones A.P., Peckett A. Zirconium-bearing aegirines from Motzfeldt, South Greenland // Contrib. Mineral. Petrol. **1980**. Vol. 75. P. 251–255.

Kato T., Murakami N. The crystal structure of kataymalite // Mineral. Journ. **1985**. Vol. 12. N 5. P. 206–217.

Konev A.A., Vorobyov E.I., Lazebnik K.A. Mineralogy of the Murunsky alkaline massif. Novosibirsk: SO RAS (Rus. Acad. Sci., Siberian Depart.). **1996**. 221 c (in Russian).

Kozlova P.S. Miserite from the Talass Alatau // Trudyi Mineral. Muzeya (Transac. Miner. Museum). AN SSSR. **1962**. Vol. 13. P. 198–204 (in Russian).

Kravchenko S.M., Bykova A.V. Miserite from South Yakutia. Mineralogy of pegmatites and gydrothermalites of alkaline massifs. M.: Nauka. **1967**. P. 160–167 (in Russian).

Krivovichev V.G. Mineralogical dictionary. SPb.: Sankt-Peterb. Univ. **2008**. 556 p (in Russian).

Kupriyanova I.I., Vasilyeva Z.V. On rare-earth miserite // Geologia mestorozhdenii redkih elementov (Geology of rare elements depositions). **1961**. Vol. 9. Novye dannye po mineralogii mestorozhdenii redkih elementov (New data on mineral of rare elements depositions) P. 139–148 (in Russian).

Lazebnik K.A., Lazebnik Yu.D. Rare silicates – miserite, canasite and fedorite in charoite rocks // Mineralogia i geokhimia ultraosnovnykh i osnovnykh porod Yakutii (Mineralogy and geochemistry of the ultra-basic and basic rocks of Yakutia). Yakutsk. **1981**. P. 32–50 (in Russian).

Linthout K. Alkali-zirconosilicates in peralkaline rocks // Contrib. Miner. Petrol. **1984**. Vol. 86. N 2. P. 155–158.

Marks M., Vennemann T., Siebel W., Markl G. Quantification of magmatic and hydrothermal processes in a peralkaline syenite – alkali granite complex based on textures, phase equilibria, and stable and radiogenic isotopes // Journ. Petrol. **2003.** Vol. 44. P. 1247–1280.

Mayorov I.P., Gavrilin R.D. Carbonatites from the Upper Paleozoic geosyncline of Turkestano-Alay // Soviet geology (Sovetskaya gelogia). **1971**. № 10. P. 111–116 (in Russian).

Menchetti S., Sabelli C. The crystal structure of baratovite // Amer. Mineral. **1979**. Vol. 64. N 3–4. P. 383–389.

Minerals. Handbook. Vol. IV. Issue 3. Silicates. Additions to volumes III and IV. M.: Nauka. **1996**. 426 p (in Russian).

Moskvin A.V. Alkaline rocks of the Hodzha-Achkan riverhead // Pamirskaya expeditsya 1930. Trudyi expeditsii (Pamir expedit. of 1930. Transac. of expedit.) L.: Academy of Sciences of the USSR. **1932**. Vol. 4/14. P. 1–99 (in Russian).

Moskvin A.V., Saukov A.A. Alkaline rocks from the river Dzhury-say in the southern Fergana // TPE 1928. Trudy exped. (Tadjik-Pamir expedit. of 1928. Transac. of expedit.). L.: Academy of Sciences of the USSR. **1931**. Vol. 7. P. 5–15 (in Russian).

Murakami N., Kato T., Hirowatari F. Katayamalite, a new Ca-Li-Ti silicate mineral from Iwagi Islet, Southwest Japan // Mineral. Journ. **1983**. Vol. 11. N 6. P. 261–268.

Murakami N. Sugilite, a new silicate mineral from Iwagi Islet, Southwest Japan // Mineral. Journ. **1976**. Vol. 8. N 2. P. 110–121.

Nenakhov V. M., Abakumova L.N., Kuznetsov L.V., Khrestenkov P.A. Legend of intrusive magmatism of the Pamiro-Alay (explanatory note). Osh: South-Kirg. Geol.-prospect. Exped. **1987**. 395 p. (in the capacity of manuscr.)(in Russian).

Oberti R., Ottolini L., Camara F., Della Ventura G. Crystal structure of non-metamict Th-rich hellandite-(Ce) from Latium (Italy) and crystal chemistry of the hellandite-group minerals // Amer. Mineral. **1999**. Vol. 84. N 5–6. P. 913–921.

Oberti R., Ventura G.D., Ottolini L., Hawthorne F.C., Bonazzi P. Re-definition, nomenclature, and crystal-chemistry of the hellandite group // Amer. Mineral. **2002**. Vol. 87. N 5–6. P. 745–752.

Omelyanenko B.I. Infiltration metasomatical zonality in postmagmatic derivates of alkaline intrusions of the Hodzha-Achkan riverhead // Fiziko-khimicheskie problemyi formirovaniya gornyh porod i rud (Phis.-chem. probl. of rocks and ores

form). M.: Nauka. **1961**. P. 525–545 (in Russian).

Omelyanenko B.I. Role of processes of assimilation and contamination in formation of the Hodzha-Achkan alkaline massif (Central Asia) // Voprosy magmatizma Srednei Azii, Kavkaza i Kazahstana (Questions of magmatism of Central Asia, Caucasus and Kazakhstan). Tr. IGEM AN SSSR. **1960**. Vol. 27. P. 39–55 (in Russian).

Omelyanenko B.I. The phenomena of a sodium metasomatose in a near-contact parts of alkaline massifs of the Hodzhaachkan riverhead // Tr. IGEM AN SSSR. **1958**. Vol. 21. P. 198–204 (in Russian).

Omelyanenko B.I., Sirotinina N.A. Accessory minerals in alkaline rocks of the Hodzha-Achkan riverhead // Materialy po geologii rudnykh mestorozhdenij, petrographii, mineralogii i geokhimii (Mater. on geology of ore fields, petrography, mineralogy and geochemistry). **1959**. M.: AN SSSR. P. 414–422 (in Russian).

Pautov L.A., Agakhanov A.A., Karpenko V.Yu., Gafurov F.G. Aleksandrovite $KLi_3Ca_7Sn_2[Si_6O_{18}]_2F_2$ – a new tin mineral // New data on minerals. **2010**. Vol. 45. P. 5–16 (in Eng.).

Pautov L.A., Agakhanov A.A., Sokolova E.V., Kabalov Yu.K. Turkestanite – a new mineral $Th(Ca,Na)_2(K_{1-x})Si_8O_{20}•nH_2O$ with a dual fourfold silicon-oxygen rings // Zap. VMO. **1997**. Vol. 126. № 6. P. 45–55 (in Russian).

Pautov L.A., Khvorov P.V. Bazirite from Tajikistan // Zap. VMO. **1998**. Vol. 127. № 1. P. 80–83 (in Russian).

Pekov I.V. Genetical mineralogy and crystal chemistry of rare elements in the high-alkaline postmagmatic systems. Doctoral dissertation. M.:MGU. **2005**. 652 p. (in Russian)

Pekov I.V., Pasero M., Yaskovskaya A.N., Chukanov N.V., Pushcharovsky D.Yu., Merlino S., Zubkova N.V., Kononkova N.N., Men'shikov Y.P., Zadov A.E. Fluorcalciobritholite, $(Ca,REE)_5[(Si,P)O_4]_3F$, a new mineral: description and crystal chemistry // Eur. J. Mineral. **2007**. Vol. 19. N 1–2. P. 95–103.

Perchuk L.L. Physico-chemical petrology of the granite and alkaline intrusions of Central Turkestano-Alai. M.: Nauka. **1964**. 244 p. (in Russian)

Perchuk L.L., Omelyanenko B.I., Shinkarev N.F. A phase and facies of alkaline intruzive of the Hodzhaachkan river basin (Alaisky ridge) in connection with questions of their genesis // Izv. AN SSSR. Ser. geol. **1961**. № 12. P. 13–23 (in Russian).

Piilonen P.C., McDonald A.M., Lalonde A.E. The crystal chemistry of aegirine from Mont Saint-Hilaire, Quebec // Canad. Mineral. **1998**. Vol. 36. N 3. P. 779–791.

Povarennykh A.C. Infrared spectrums of a ring silicates // Miner. Zhurn. **1979**. Vol. 1. № 2. P. 3–18 (in Russian).

Pyatenko Yu.A., Kurova T.A., Chernitsova N.M., Pudovkin Z.V., Blinov V.A., Maximova N.V. Niobium, tantalum and zirconium in minerals. M.: IMGRE. **1999**. 213 p. (in Russian)

Reguir E.P., Chakhmouradian A.R., Evdokimov M.D. The mineralogy of a unique baratovite and miserite-bearing quartz-albite-aegirine rock from the Darai-Pioz complex, Northern Tajikistan // Canad. Mineral. **1999**. Vol. 37. N 6. P. 1369–1384.

Rozhdestvenskaya I.V., Evdokimov M.D. Refinement of crystal structure of miserite $(K_{1.29}\square_{0.21})[Ca_{5.5}M^{3+}{}_{0.49}](Si_6(O,OH)_{15}(Si_2O_7)(F,OH)_2•0.25H_2O$ (M = Y, TR, Fe, Ti, Mn, Mg, Na) from the Darai-Pioz deposition, Pamir, Tajikistan // Dokl. AN. **2006**. Vol. 406. № 2. P. 236–240 (in Russian).

Ryzhev B.I., Moleva V.A. A find of miserite in the USSR // Dokl. AN SSSR. **1960**. Vol. 131. № 6. P. 1420–1422 (in Russian).

Sandomirsky P.A., Simonov M.A., Belov N.V. The crystal structure of baratovite $KLi_3Ca_7Ti_2[Si_6O_{18}]_2F_2$ // Dokl. AN SSSR. **1976**. Vol. 231. P. 615–618 (in Russian).

Schaller W.T. Miserite from Arkansas; a renaming of natroxonotlite // Amer. Mineral. **1950**. Vol. 35. N 9–10. P. 911–921.

Scott J.D. Crystal structure of miserite, a Zoltai type 5 structure // Canad. Mineral. **1976**. Vol. 14. P. 515–528.

Semenov E.I., Dusmatov V.D. Agrellite – the first find in the USSR // Mineralogiya Tadjikistana. **1989**. Vol. 8. P. 3–6 (in Russian).

Semenov E.I., Dusmatov V.D., Khomyakov A.P. About rare-earth miserite // Mineralogicheskie issledovania. M.: IMGRE. **1973**. Vol. 3. P. 42–45 (in Russian).

Shinkaryov N.F. The upper Paleozoic magmatism of the Turkestano-Alai. L.: LGU (Leningrad State Univers.). **1966**. 150 p. (in Russian)

Sidike A., Kobayashi S., Zhu H.-J., Kusachi I., Yamashita N. Photoluminescence of baratovite and katayamalite // Phys. and Chem. Miner. **2010**. Vol. 37. Issue 10. P. 705–710.

The stratified and intrusive formations of Kirgizia. Frunze: Ilim. **1982**. Book 2. 245 p. (in Russian).

Tsareva G.M., Kartashov P.M., Dubrovinsky L.S., Kovalenko V.I. About gittinsite from rare-metal alkaline granites of the Western Mongolia // Dokl. AN. Ser. geologia. **1993**. Vol. 331. № 1. P. 82–86 (in Russian).

Ul'yanov T.P., Ilyinsky G.A. New data on miserite from the Hodzhaachkan (Alaysky ridge) // Mineralogiya i geokhimiya. L.: LGU (Leningrad State Univers.). **1964**. Vol. 1. P. 40–45 (in Russian).

Weber V.N. Geological map of Central Asia. Sheet VII – 6 (Isfara), northern part // Trudyi Vsesoyuznogo geologo-razvedochnogo ob'edinenija NKTP SSSR (Transact. Rus. geol.-prospect. Assoc. NKTP USSR). Issue 194. L.-M.-Novosibirsk: State Sci.-tech. mining-geol.-petrol. publish. house. **1934**. 278 p. (in Russian).